

ABOVE GROUND MANGROVE FOREST BIOMASS AND CARBON STOCK ASSESSMENT WITH TERRESTRIAL LASER SCANNER USING QUANTITATIVE STRUCTURE MODEL

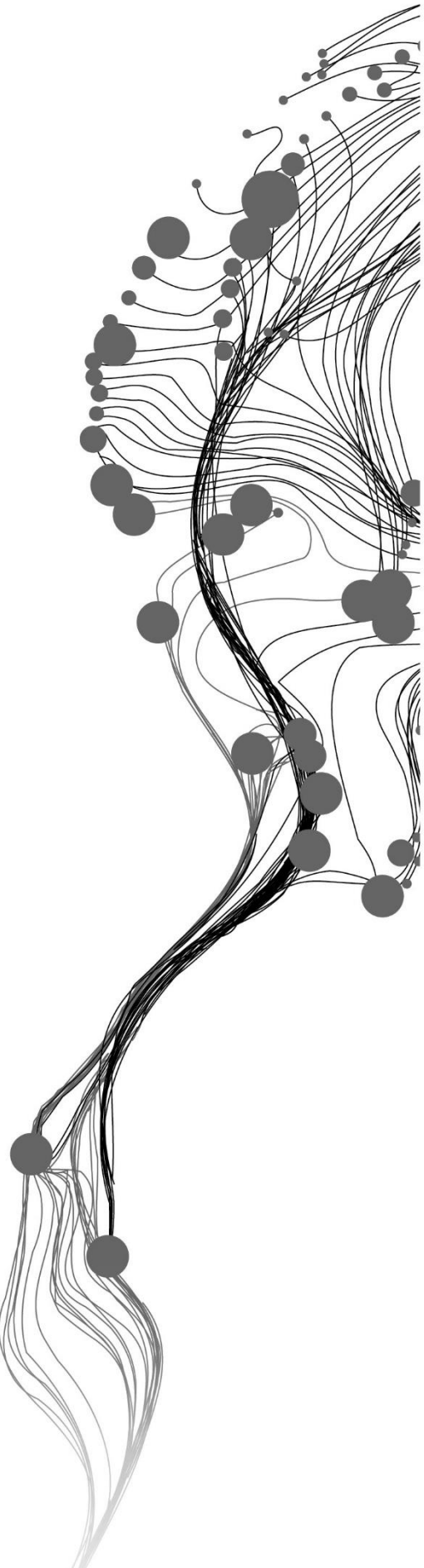
GEZAHEGN KEBEDE BEYENE
FEBRUARY, 2019

SUPERVISORS:

Dr. Y. A. Hussin
Dr. Iris van Duren

ADVISOR:

Dr. Y. Budi Sulistoadi (University of Mulawarman, Samarinda, Indonesia)



Above Ground Mangrove Forest Biomass and Carbon Stock Assessment with Terrestrial Laser Scanner Using Quantitative Structure Model.

GEZAHEGN KEBEDE BEYENE

Enschede, The Netherlands, FEBRUARY, 2019

Thesis Submitted to the Faculty of Geo-Information Science and Earth Observation of the University of Twente in partial fulfilment of the requirements for the degree of Master of Science in Geo-Information Science and Earth Observation.

Specialization: Natural Resources Management

SUPERVISORS:

Dr. Y. A. Hussin

Dr. Iris van Duren

ADVISOR:

Dr. Y. Budi Sulistoadi (University of Mulawarman, Samarinda, Indonesia)

THESIS ASSESSMENT BOARD:

Dr. Ir. C.A.J.M. de Bie (Chair)

Dr. T. Kauranne (External Examiner, LUT School of Engineering Science, Finland)

DISCLAIMER

This document describes work undertaken as part of a programme of study at the Faculty of Geo-Information Science and Earth Observation of the University of Twente. All views and opinions expressed therein remain the sole responsibility of the author, and do not necessarily represent those of the Faculty.

ABSTRACT

Mangroves are highly valuable green vegetation types that enhance ecological diversity in the coastal areas and support socio-economic activities (Nagelkerken et al., 2008). From the total world mangroves, Indonesian share is 22.6% which is around 3.11 million ha area coverage, and it is a home of diversified species (Giri et al., 2011). With its biological importance and productivity, mangroves are a unique ecosystem that provides goods and services to society (Giri et al., 2011). However, the rate at which mangroves degraded and disappeared have enormous consequences on the aquatic ecosystems, atmospheric condition and climate (Giri et al., 2011). Climate change is significantly affected by the most predominant Green House Gases (GHGs) which is CO₂ emission (Palacz et al., 2013).

In most cases, estimation of above ground biomass/carbon stock relies on allometric equations. Application of terrestrial laser scanner (TLS) using quantitative structural model (QSM) focus on common areas such as the inland forest. In this study, we used TLS to estimate above ground biomass (AGB) of mangrove forest in the coastal area using QSM which is independent of diameter at breast height (DBH). We also evaluate the tree parameters, DBH and height derived from TLS with field measured DBH and height. The DBH and tree height from TLS showed high agreement with DBH and height from field with R² 0.978 and RMSE of 0.62 cm, and R² 0.73 with RMSE of 1.93 m respectively. The tree parameters (DBH and height) that measured in the field were used to estimate AGB/carbon stock using allometric equation derived by Chave et al. (2005) and used as a reference to AGB/carbon stock derived from TLS and QSM.

Above ground biomass of 115 trees were derived from TLS and QSM compared with AGB estimated from the field measured in the Delt of Mahakam River, East Kalimantan, Indonesia. The point clouds generated using TLS, were registered and filtered to produce separate point clouds for individual trees. Trees extracted from the TLS point cloud data were used to estimate the tree volume using QSM. For reconstruction of trees in QSM, trees with dense point cloud from TLS were selected. The visible part of the tree reconstructed by a cover with a cylinder and AGB estimated from cylinder volume. The AGB derived from these volumes and wood density compared with AGB from allometric equations using field-measured tree parameters. The AGB from TLS using QSM show a high agreement with the reference values from field measured AGB with a coefficient of determination (R²) 0.965 and RMSE of 21.08 kg/tree, and high correlation between AGB estimated from the field and derived from TLS with R² 0.978 and RMSE of 14.49 kg/tree. In general, there were no significant differences observed in both methods of estimating AGB. The result shows that point cloud that generated from TLS can effectively be used in QSM to assess AGB/carbon stock of mangrove forest in the coastal area.

Keywords: Aboveground biomass, Carbon stock, Terrestrial laser scanner, Quantitative structure model, Allometric equation.

Dedicated to my wife, Mrs. Abeba Leta, for her encouragement, support, love and take care of my children.

ACKNOWLEDGEMENTS

My utmost gratitude is to Almighty God for all what he has done for me throughout this journey of my M.Sc.

I am very grateful to express my gratitude to my first supervisor Dr. Yousif Ali Hussin for his patience, motivation, enthusiastic, valuable comments, continuous and tremendous support from the early beginning till the end of this research. It was a great opportunity and pleasure to work under Dr. Yousif Ali Hussin supervision. His door is always open, and he all the time has a welcoming face. I sincere gratitude my second supervisor Dr. Iris Van Duren for her valuable and critical comment, tremendous support and hard questions were extremely helpful and improved the quality of my research.

My sincere thanks to Dr. Ir. Cees de Bie for his constructive and valuable comments during the proposal and mid-term defences. I am very much grateful to Drs. Raymond Nijmeijer for his help and motivation since the beginning of the course until the end of this study.

Special thanks to the University of Mulawarman, the Faculty of Forestry, Dr. Y. Budi Sulistioadi for all their support in facilitating the field work, helping with the logistics. Special thanks go to Mr. Rafii Fauzan, Mr. Lutfi Hamdani and Mrs. Meta Priskawanti for their help during field data collection in mangrove forest to identify suitable plots, clearing undergrowth and recognising tree species.

My sincere gratitude goes to Dr. Pasi Raunonen for the right to use the QSM algorithm and technical assistance concerning the use of the algorithm, and I appreciate the speedy response to my questions.

I want to present sincere thanks to my fieldwork mates Weday Berhe, Eko, Mahmud, Hashem, and Karimon. Thanks to NRM classmates for fruitful time and joyfulness throughout the 18 months we stay together. I am very appreciative to my friends Bililign Deresse, Samson and Mulugeta for their support and quality time spent together during the stay in the Netherlands.

Last but not least to my family. I want to express my deeply grateful to my beloved wife, children, father, mother, sister, and brothers for their unconditional love, patience and encouragement throughout my study. They have been a source of my inspiration, and without them, this accomplishment would not have been possible. Thank you.

Gezahegn Kebede Beyene
Enschede, The Netherlands
February 2019

TABLE OF CONTENTS

Abstract	iii
List of figures.....	viii
List of tables	ix
List of acronyms.....	x
1. INTRODUCTION	1
1.1. Background.....	1
1.2. Problem statement.....	3
1.3. General Objective.....	4
1.4. Specific objective	4
1.5. Research Questions.....	4
1.6. Research Hypothesis.....	4
1.7. Conceptual Diagram.....	5
1.8. Literature Review.....	6
1.8.1. Terrestrial Laser Scanner	6
1.8.2. Biomass/carbon stock estimation	6
1.8.3. Quantitative Structure Model (QSM)	7
1.8.4. Allometric Equations	7
2. Study Area, Materials and Methods	8
2.1. Description of the study area.....	8
2.1.1. Climate and Vegetation	9
2.2. Materials.....	9
2.2.1. Field equipment.....	9
2.2.2. Software	9
2.3. Methods.....	9
2.3.1. Sampling Design and determination of sample plot	10
2.3.2. Terrestrial Laser Scanner plot arrangement	11
2.3.3. Centre plot identification, tree labelling and undergrowth clearing.....	11
2.4. Terrestrial Laser Scanner data acquisition	12
2.4.1. Retroreflector.....	12
2.4.2. Terrestrial Laser Scanning	13
2.5. Biometric data collection.....	14
2.6. Pre-processing of point cloud.....	15
2.6.1. Scanning position registration	15
2.6.2. Extraction of individual tree.....	15
2.7. Tree parameters extraction and measurement.....	16
2.8. Conversion of point clouds into ASCII format and QSM.....	17
2.8.1. Filtering of point clouds.....	17
2.8.2. Optimisation of input parameters in QSM.....	19
2.8.3. Steps of the reconstruction process	21
2.8.4. Cover sets.....	21
2.8.5. Tree Components	22
2.8.6. Segmentation	22
2.8.7. Cylinder reconstruction.....	23
2.8.8. Completing the cylinder model.....	23

2.8.9. Tree characteristics	23
3. Result.....	24
3.1. Descriptive Statistics.....	24
3.1.1. Diameter at Breast Height (DBH) measurement	24
3.1.2. Height measurement.....	25
3.1.3. Mangrove forest tree species.....	25
3.2. The relationship between TLS derived, and field measured DBH and height	26
3.3. The relationship between TLS obtained, and field measured DBH and height	27
3.3.1. Above ground biomass estimated using field-measured tree parameters	27
3.3.2. Above ground biomass derived from TLS point clouds	27
3.3.3. The relationship between AGB from TLS point clouds and field-measured tree parameters...27	
3.3.4. Testing the relationship between AGB from TLS and field-measured tree parameters	28
3.3.5. Above ground biomass derived from QSM	28
3.3.6. The Relationship between AGB derived from QSM and field measured AGB.....	29
3.3.7. Testing the Relationship between AGB derived from QSM and field measured	30
3.3.8. The Relationship between AGB derived from QSM and TLSpoint clouds	30
4. Discussion.....	32
4.1. Application of Quantitative Structure Model (QSM) to Estimate AGB in Mangrove Forest.....	32
4.2. DBH measurement and sources of error.....	32
4.2.1. Distribution of field measured DBH, and TLS derived DBH	34
4.3. Tree height measurement accuracy and source of error.....	34
4.4. Acquisition and Registration of point clouds.....	35
4.5. Individual tree extraction.....	36
4.6. Wood density	36
4.7. Above Ground Biomass/Carbon Stock Accuracy Assessment test	37
4.7.1. Field measured AGB compared with AGB derived from TLS	37
4.7.2. Field measured AGB compared with AGB derived from QSM.....	37
4.7.3. Above ground biomass derived from QSM compared with AGB derived from TLS	38
5. Conclusion and recommendation	39
5.1. Conclusion.....	39
5.2. Recommendation.....	40
References.....	41
List of Appendices.....	46

LIST OF FIGURES

Figure 1. A conceptual diagram -----	5
Figure 2. TLS mounted on a tripod and scan tree structure -----	6
Figure 3. Map of the study area in Angan district -----	8
Figure 4. Flow chart of the research methods -----	10
Figure 5. Tree labelling to identify trees in the sample plot -----	11
Figure 6. Multiple TLS scanning position -----	12
Figure 7. Both circular and cylindrical retroreflectors -----	13
Figure 8. TLS Levelling setup -----	13
Figure 9. <i>Rhizophora</i> species that need to climb them to measure DBH -----	14
Figure 10. The procedure that shows how to register the different scanning positions -----	15
Figure 11. Manually extracted individual tree -----	16
Figure 12. Individual tree DBH measured from manually extracted point clouds -----	16
Figure 13. Individual tree height measured from extracted point clouds -----	17
Figure 14. Extracted individual tree before filtering and after filtered -----	18
Figure 15. A segmented tree structure and fitted to the cylinder -----	20
Figure 16. Main steps of reconstruction a tree using QSM -----	21
Figure 17. Minimum cover set 2cm (left) and maximum cover set 10cm (right) -----	22
Figure 18. Filling gap to reconstruct the whole structure of a tree -----	23
Figure 19. Field measured DBH, and TLS derived DBH -----	24
Figure 20. Distribution of field measured tree height (left) and TLS derived height (right) -----	25
Figure 21. The dominant mangrove tree species in area -----	25
Figure 22. The relationship between field measured, and TLS derived DBH -----	26
Figure 23. The relationship between field-measured height and TLS derived height -----	26
Figure 24. The relationship between field-measured AGB and TLS derived AGB -----	28
Figure 25. AGB derived from TLS was highly correlated with field measured AGB -----	28
Figure 26. The AGB derived from QSM and field measured AGB using specific wood density -----	29
Figure 27. Above ground biomass derived from QSM and ABG estimated from field measured. -----	29
Figure 28. The relationship between AGB derived from QSM and derived from TLS -----	30
Figure 29. The relationship between TLS and QSM derived AGB using specific wood density. -----	31
Figure 30. Mangrove forest with prop roots that challenges measuring the diameter -----	33
Figure 31. TLS derived DBH through circular fitting method -----	34
Figure 32. Young and open canopies of mangrove forest -----	35
Figure 33. Bottom view (left) and top view (right) manually extracted individual trees -----	36
Figure 34. Closed canopy tropical forest (left) and young open mangrove forest (right). -----	37

LIST OF TABLES

Table 1. Field equipment used for biometric data collection and tree scanning.	9
Table 2. Software used for data processing analysis.	9
Table 3. TLS scanner setting used during the field work.	14
Table 4. Descriptive statistics of above ground biomass from field measured using generic and specific wood density.	27

LIST OF ACRONYMS

3D	Three Dimensions
AGB	Above Ground Biomass
DBH	Diameter at Breast Height
FAO	Food and Agricultural Organization
GHHs	Green House Gasses
IPCC	Intergovernmental Panel on Climate Change
LiDAR	Light Detection and Ranging
MRV	Measurement Reporting and Verification
QSM	Qualitative Structural Model
REDD ⁺	Reducing Emission from Deforestation and Degradation
RMSE	Root Mean Square Error
SWD	Specific Wood Density
TLS	Terrestrial Laser scanner
UN	United Nation

1. INTRODUCTION

1.1. Background

Mangroves are highly valuable green vegetation types that enhance ecological diversity in the coastal areas and support socio-economic activities (Nagelkerken et al., 2008). According to Tomlinson (1994), Mangroves defined as “association of trees and shrubs forming the dominant vegetation in tidal, saline wetlands, along equatorial, tropical and subtropical coasts.” The global estimation of mangrove forests coverage estimated by Giri et al. (2011) is 137,760 km² which is less by 12.35% than that predicted by FAO (2007). From total world mangroves, Indonesian share is 22.6% which is 3,112,989ha area coverage, and it is a home of diversified species (Giri et al., 2011).

With its biological importance and productivity, mangrove is a unique ecosystem with many goods and services that provide to the society, as well as its well known coastal and marine ecosystem (Giri et al., 2011). Mangroves stabilise and minimise the overwhelming effect of natural disasters like tsunamis, cyclones, hurricanes, and storms. Likewise, the existence of mangrove forest provides breeding and nursing habitat for aquatic and pelagic species, and a good source of food, medicine, fuel and construction materials for local societies (Giri et al., 2011). Among the tropical ecosystems, mangroves are the most carbon-rich forest, and their carbon fraction is significantly plant-derived (Kristensen et al., 2008) and has a potential of more than three to four (3-4) times carbon as compared to the tropical forest (Donato et al., 2011). The efficiencies of mangroves to trap suspended materials from the aquatic ecosystem and its influence on the universal carbon budget is high (Dittmar et al., 2006). Furthermore, Mangrove forests show an essential role in sequestering and storing blue carbon (Duarte et al., 2013).

Despite their importance and significance in providing ecological, social and economic services to the community, mangroves are the most threatened ecosystem habitat in the tropics (Valiela et al., 2001). The rate at which mangroves deforested is considerably high as compared to world forest deforestation (FAO, 2007). As long as the current trend of deforestation continues the prediction shows that, we will lose 30-40% of wetland and 100 % of the mangroves (Duke et al., 2007) in the coming 100 years. As a consequence, vital ecosystem goods and services like the natural barrier of tsunami and hurricanes, carbon sequestration and biodiversity services provided by mangrove forests will diminish (Bouillon et al., 2008). In the last six centuries, the mangroves habitat of Indonesia has declined by more than 70% (Duarte et al., 2013). The significant contributors to mangroves habitat loss in Indonesia are a brackish pond and timber exploitation.

The rate at which mangroves degraded and disappeared have enormous consequences on the marine ecosystems, atmospheric condition and climate (Giri et al., 2011). The effect of climate change on the environment makes a regularly growing requirement for precise 3D information on the entire planet earth (Dassot et al., 2011). Climate change is significantly affected by the most predominant Green House Gases (GHGs) which is CO₂ emission (Palacz et al., 2013). Virtually, the consequence of climate change has increased primarily in the coastal area (Alongi, 2008). However, mangrove forest has the potential to sequester approximately 22.8 million metric tons each year (Giri et al., 2011). Forest productivity, carbon storage, and sequestration are determined based on the above-ground biomass (AGB) (Bienert et al., 2006). According to Houghton et al. (2009) the availability of sinks and distributions of carbon sources is uncertain, and the level of emissions at local, national and global scales are poorly known. Remote sensing techniques offer opportunities for mapping the biophysical and structural parameters of mangroves with speed and reduce uncertainty in estimates of biomass and carbon stocks (Pham et al., 2019).

Based on REDD+, the developing countries can reduce emissions from deforestation and forest degradation, by implementing either sustainable forest management, avoiding deforestation, avoiding forest degradation, conserving or enhancing forest carbon stock (FAO, 2017). To be able to claim the financial benefit for reduced carbon emission, the countries are required to present the proof of increased biomass/carbon stock in their forests. Several methods have been proposed to achieve quantifying the change in forest biomass/carbon stock (The REDD Desk, 2017).

Measuring Reporting and Verification (MRV) is the mechanism that REDD+ program is proposing to all countries, for which it recommends the use of different remote sensing techniques such as very high-resolution satellite images, SAR images (backscatter) and Lidar to assess aboveground biomass and carbon stock (FFPRI, 2012). Several studies have been used allometric equations to measure AGB/carbon stock. According to Coronado et al. (2004) “crown area, some prop roots, and total tree height” have been used to estimate the AGB of mangroves. A study by Smith & Whelan (2006) showed that DBH and tree height are excellent interpreters for AGB. Chave et al., (2005) also indicated that DBH and wood specific density could be used to develop an allometric equation that estimates AGB.

Measuring tree biomass/carbon stock helps to estimate the role of forest in the regional and global carbon cycle (Zianis, 2008). However, accurate measurement and monitoring of mangrove forests are essential to estimate carbon stock/biomass dynamics and management of the ecosystems (Houghton et al., 2009; Næsset et al., 2004). But, there is inconsistency in the estimation of aboveground biomass (AGB) and carbon stock globally, which related to single tree biomass estimation (Mitchard et al., 2014), because, estimation of vegetation biomass is not directly measured by remote sensing (RS) which may lead to missing significant spatial variation in forest structure.

Terrestrial Laser Scanning (TLS), also known as terrestrial LiDAR (light detection and ranging), is an active remote sensing technology that allows capturing high resolution three dimensional (3D) point cloud structure of trees with relatively time and energy saving (Adewole et al., 2016). The benefit of TLS in forest inventory is to improve the work efficiency in the sampling plots by replacing manual measurements of tree attributes (Vastaranta et al., 2009). TLS can determine high-quality tree attributes that are important in determining the biomass/carbon stock of trees with high accuracy level (Yu et al., 2013). The capability of TLS in capturing 3D makes it recommendable in the assessment of forest environment (Krooks et al., 2014). It has been extensively used to study forest inventory (Liang et al., 2016) in detecting tree species (Othmani et al., 2013), estimating leaf area (Béland et al., 2014) and modelling small trees (Hess et al., 2015). But there are a few studies conducted to estimate biomass/carbon stock of mangrove forest using TLS ((Feliciano et al., 2014).

The problem related to the development of allometric equations to estimate AGB could accurately fix by using Terrestrial LiDAR (Light Detection and Ranging). TLS can generate a point cloud of trees with detailed data needed to estimate AGB (Feliciano et al., 2014). According to Raunonen (2015), AGB is not equal in all parts of the tree which makes it difficult to assess the AGB of individual biomass/carbon stock accurately. To cope up with inaccuracies of AGB/carbon stock measured, TLS measurements using 3D Quantitative Structural Model (QSM), which accurately capture the structure of the trees is essential. Therefore, this research intends to estimate the amount of AGB/carbon stock stored in different parts of mangrove trees using 3D QSM and combine them to get biomass/carbon stock particularly on the base of the individual tree.

1.2. Problem statement

Mangrove forest is a unique ecosystem that provides enormous goods and services to the local and global community (Giri et al., 2011). But, to give information on mangroves forest ecosystems, it requires a lot of data which are difficult to assess directly (Olschofsky et al., 2016). However, mangrove forest biomass/carbon stock is the one that needs estimating accurately to indicate its role in global climate change mitigation. As the potential of mangrove forest in carbon sequestration is high compared to the tropical inland forest, estimating AGB/carbon stock of mangroves are essential. Accordingly, an accurate measurement of diameter at breast height (DBH) and tree height are the basis for assessment of AGB/carbon stock (Köhl, 2006) and desirable for sustainable forest resource planning (Pretzsch, 2009), which is strongly linked to biomass and carbon stock of the forest (Yu et al., 2013).

Even though forest parameters are critical to model biomass/carbon stock of the forest, but inaccurate measurement leads to overestimation or underestimation of AGB/carbon stock (Næsset et al., 2004). Allometric equations which convert tree height and DBH to biomass/carbon stock directly is uncertain, because, it depends on the capability of the equation to manage variation (Chave et al., 2014) and difference of biomass/carbon stock in different parts of the tree (Raumonen, 2015).

According to Zianis & Seura (2005) “The simplified statistical models are limited in accuracy, and cannot give accurate quantitative and geometric information on a single tree, especially in the branch level.” As Newnham et al. (2016) showed Terrestrial Laser Scanning “presents an opportunity to go beyond simple empirical isometric and allometric equations to the point where three-dimensional measurements could use as a basis for assessing tree volume,”.

Terrestrial Laser Scanner can determine high-quality tree attributes that are important in estimating biomass with high accuracy level (Yu et al., 2013). From TLS point cloud branch distribution can be reconstructed using QSM algorithms (Raumonen et al., 2013). Combining TLS with QSM provides a detailed structure of the trees that enables us to estimate biomass (Krooks et al., 2014). The improvement of methods to assess AGB/carbon stock of forest accurately shows the specific implication of considering an increase in the importance of AGB assessments and forest carbon stock inventories (IPCC, 2006).

Assessment of AGB/carbon stock by TLS using QSM applied in the tropical inland forest, but there is no work done yet on the evaluation of mangrove forest AGB by TLS using QSM. A study conducted to estimates AGB of mangrove forests using TLS (without QSM) done at Everglades National Park, Southwestern coast of South Florida (Feliciano et al., 2014) showed that TLS is a promising option for non-destructive sampling to measure AGB. However, estimating AGB in tropical mangroves by TLS using QSM is entirely new. We do not know yet if and to what extent TLS using QSM can improve the accuracy of biomass and carbon estimates. Therefore, this research is aiming at assessing the applicability of TLS using QSM to estimate AGB in tropical mangroves of the Delta of Mahakam River, East Kalimantan, Indonesia.

1.3. General Objective

Primarily this research aims to estimate AGB/carbon stock with TLS using 3D Quantitative Structure Model (QSM) in tropical mangrove forests of the Delt of Mahakam River, East Kalimantan, Indonesia.

1.4. Specific objective

The specific objectives of this research are:

1. To assess the relation between DBH and height measured in the field and derived from TLS.
2. To compare the accuracy of biomass/carbon stock derived from TLS with AGB/carbon stock obtained from field measurement
3. To estimate biomass/carbon stock acquired from TLS using QSM
4. To compare the accuracy of biomass/carbon stock obtained from field measurement with biomass/carbon stock acquired from TLS using QSM

1.5. Research Questions

1. What is the relation between height and DBH estimated from field measurement and derived from TLS?
2. How accurate is AGB/carbon stock derived from TLS compared with AGB/carbon stock estimated from field measured?
3. What is the relationship between AGB/carbon stock derived from TLS and AGB/carbon stock from QSM?
4. How accurate is AGB/carbon stock derived from TLS using QSM compared with AGB/carbon stock estimated from field-measured tree parameter by the allometric equation?

1.6. Research Hypothesis

1. **Ho:** There is no significant difference between DBH and height derived from TLS and the field measurement.
Ha: There is a significant difference between DBH and height derived from TLS and the field measurement.
2. **Ho:** There is no significant difference between AGB/carbon stock derived from TLS and the one obtained from the field measurement.
Ha: There is a significant difference between AGB/carbon stock derived from TLS and the biomass/carbon stock obtained from the field measurement.
3. **Ho:** There is no significant difference between AGB/carbon stock derived from TLS and AGB/carbon stock derive from QSM.
Ha: There is a significant difference between AGB/carbon stock derived from TLS and AGB/carbon stock form QSM
4. **Ho:** There is no significant difference between AGB/carbon stock from an allometric equation based on field-measured tree properties and AGB/carbon stock based on TLS measured tree properties using QSM.
Ha: There is no significant difference between AGB/carbon stock derived from an allometric equation based on field-measured tree properties and AGB/carbon stock based on TLS measured tree properties using QSM.

1.7. Conceptual Diagram

The conceptual diagram (Figure 1) shows the relevant interaction between different elements of the system in this research which focus on measuring mangrove tree structure by using TLS and field measuring tools such as diameter tape and Leica DISTO. The biomass/carbon stock of mangrove forest in the study area measured in line with REDD+ project techniques (i.e., MRV) that provided to the developing country to estimate the amount of carbon they sequestered using appropriate methods. Such as, application of TLS to determine the amount of forest biomass/carbon stock, which is similar to what we did in this research. Mangrove Forests in East Kalimantan, Indonesia

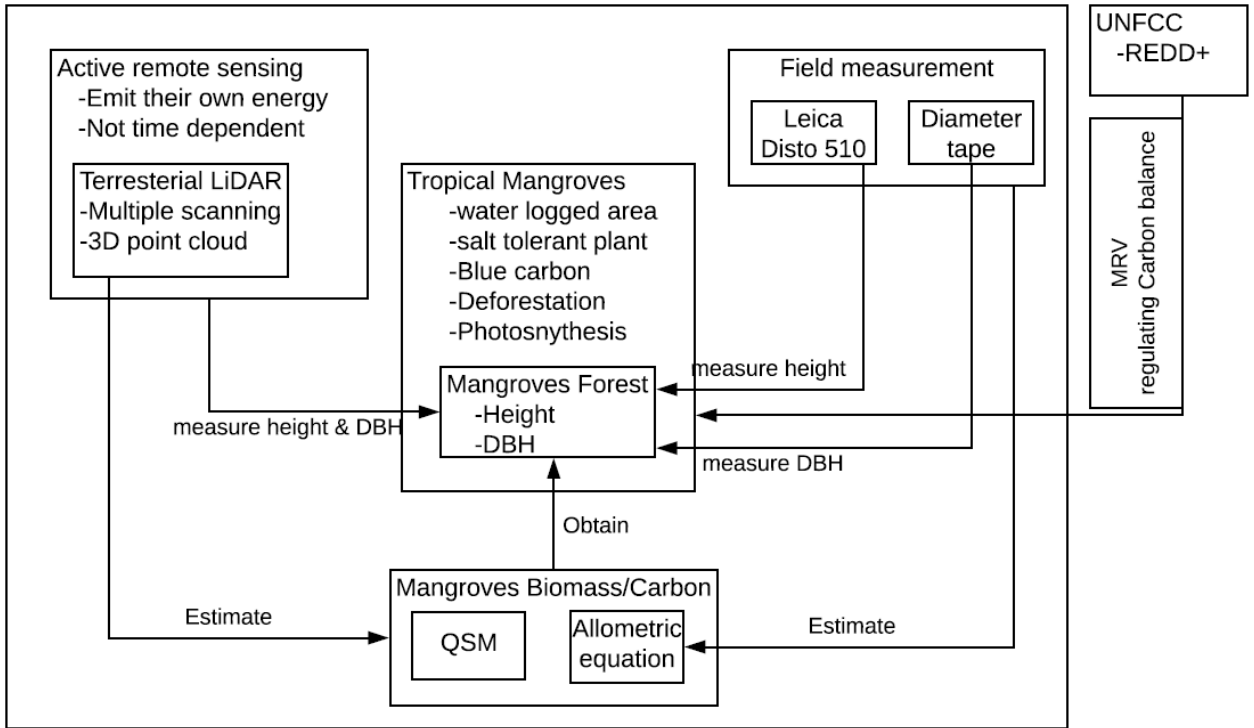


Figure 1. A conceptual diagram indicates different interaction between the mangrove forest ecosystem and tree parameters measuring using various techniques to assess AGB/carbon stock of individual trees.

1.8. Literature Review

1.8.1. Terrestrial Laser Scanner

A terrestrial laser scanner (TLS), similarly named as terrestrial light detection and ranging (LiDAR), which is a type of an active remote sensing that measures distances by transmitting laser pulses and analysis the return of energy accurately as a function of time (Newnham et al., 2016) and provides detailed information on forest structure. LiDAR can be operated from different platforms, namely the ground (terrestrial), airborne and satellite. These operating platforms provide different scales and details of forest structures that are important for forest inventory parameter estimation (Popescu et al., 2011). Laser measurements have been applied in standard surveying application instruments for the past decades to measure object structure, and in the late 1990s, manual and specific measuring mechanism was developed into an automated 3D by a terrestrial laser scanner (Liang et al., 2016).

TLS is a laser-based device that measures its surroundings using LiDAR. It generates millions of points and represents an object into a 3D structure (Wilkes et al., 2017). The techniques that used for the range measurement in laser scanning systems are phase shift (PS) and time-of-flight (TOF). Phase shift ranging makes use of continuous laser illumination, and amplitude variation of the beam to differentiate the range at high frequency and time-of-flight utilises precise timing for determining the array from the pulse time of flight and the speed of light (Liang et al., 2016). TLS is a reliable tool to assess the structure and dimension of the forest (Calders et al., 2015). measuring forest structure using TLS can provide accurate data and has the potential to decrease uncertainties in estimating AGB since it allows a direct estimate of tree volume (Figure 2)

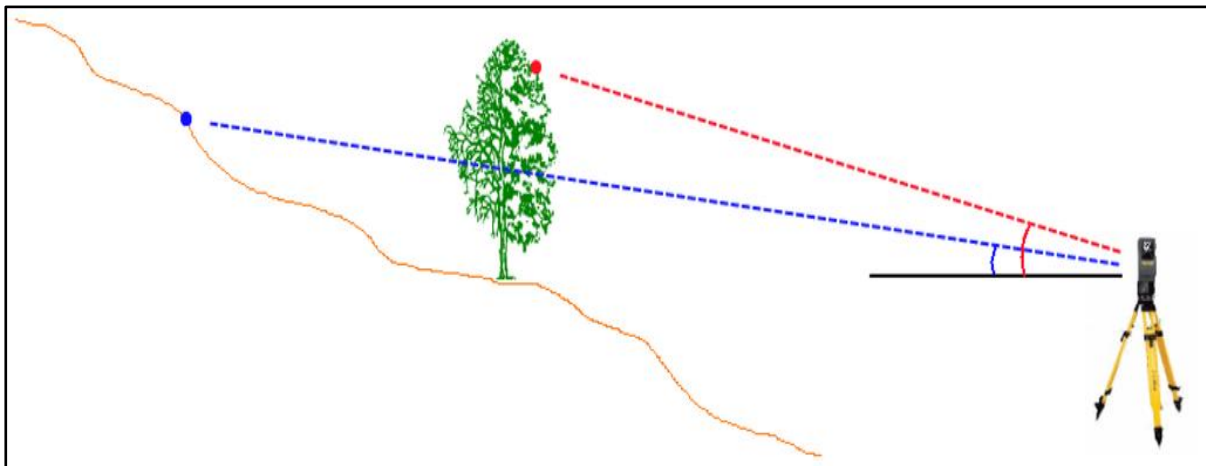


Figure 2. TLS mounted on a tripod and scan tree structure (Panholzer & Prokop, 2013)

1.8.2. Biomass/carbon stock estimation

The quantity of biological material available above the top of the soil surface which is oven-dry to remove water in a specified area called Aboveground biomass (AGB) (Drake et al., 2003). 50% of the plant dry biomass is carbon. The carbon pools of tropical forest ecosystems are biomass of the tree, understory vegetation, dead mass of litter, wood debris and soil organic carbon. From these, the carbon that stored in the aboveground biomass of a tree is typically the largest and directly impacted by deforestation and forest degradation (Gibbs et al., 2007). Direct and indirect methods can estimate aboveground biomass. The direct method of estimation requires, harvesting of the tree, dried until constant weight and weighted for estimating biomass (Gibbs et al., 2007). This method is accurate, but it is time-consuming, labour intensive and not applicable to a large area. The indirect way needs a representative sample of the area and tree parameters (DBH and height) to estimate above ground biomass of the individual tree.

Dry carbon stock is derived merely from the aboveground biomass (Basuki et al., 2009; Drake et al., 2003). Estimation of biomass/carbon stock is very significant for evaluating the productivity and sustainability of the forest (Vashum & Jayakumar, 2012). Field measurement, remote sensing, and GIS can be used to estimate forest biomass/carbon stock (Lu, 2006). AGB is an essential indicator of forest productivity, carbon storage, and sequestration (Ruiz-Peinado et al., 2012). The entire earth planet carbons sink and sources distribution are uncertain (Houghton et al., 2009) and the emission of carbon at local, national and global scales are poorly known (Hill et al., 2013). To monitor and estimate AGB/carbon stock over a large area remote sensing technique are essential (Schwieder et al., 2018), especially with the present growing curiosity in forest carbon stock change (Sy et al., 2015). Accurate ground reference measurements are intended for the calibration and validation of these global satellite-derived AGB data sets.

1.8.3. Quantitative Structure Model (QSM)

Quantitative structure Model is a method that can measure the total woody biomass of individual tree volume directly. It is a comprehensive model used for reconstructing tree structure from point cloud acquired by TLS. AGB/carbon stock derived from QSM can be estimated in a non-destructive way (Hackenberg et al., 2015) and, AGB of a single tree can be modelled as accurately as possible (Hackenberg et al., 2014). Pfeifer et al. (2004) indicate QSM is an automatic way of demonstrating the stem and branching structure of a tree. Establishing tree model from TLS-data is the method developed by Raunonen et al. (2013). The technique produces a QSM of the tree (Calders et al., 2015). This method developed by Raunonen et al. (2013) imports TLS-point clouds and reconstructs the tree as a hierarchical collection of cylinders, as described in Åkerblom et al. (2015). From QSM result, it is possible to estimate almost any geometrical, or distributions that represent a tree structure (such as stem and branch volumes and lengths).

1.8.4. Allometric Equations

Allometric equations are critical for quantifying many aspects of ecology and Forestry including the prediction of the tree and stand variables to estimate carbon stock, productivity and ecosystem services at the tree and landscape levels (Chave et al., 2014). There are two methods of field measurement available to estimate biomass, among these, the first is the destructive method which is sometimes called as harvest method which can measure biomass and carbon stock of a tree (Gibbs et al., 2007). The second is the non-destructive method that can rely on the allometric equation. Allometric equations most widely used for biomass estimation (Vashum & Jayakumar, 2012), and developed as a function of different physical tree parameters such as DBH, height, crown diameter, etc.. This method is estimating biomass and carbon stock the tree without felling, that use allometric equations which often site and species dependent (Smith & Whelan, 2006). Studies by Comley & McGuinness, (2005) offer an inclusive survey of the relevant literature. They suggest that species-specific characteristic of allometric equations, which implies that allometric equations used is significantly different among mangrove tree species. In both cases of species and site-specific (Chave et al., 2005; Komiyama et al., 2005) general allometric equations are more recommended to be used for mangroves.

$$AGB = 0.0673 * (\rho * D^2 * H)^{0.976},$$

Where,

AGB = Above Ground Biomass (kg)

D = Diameter at breast height (cm)

H = Height (m)

ρ = Specific wood density (g/cm³)

2. STUDY AREA, MATERIALS AND METHODS

2.1. Description of the study area

The location of the study area is in Mahakam delta east coast of Borneo Island specifically in the province of East Kalimantan, Indonesian, between 0°21' and 0°10' South and between 117° 15' and 117° 40' East, placed at the mouth of the Mahakam River (Bosma et al., 2012) (Figure 3). The area is slightly larger than one square kilometre and consists of a collection of islands. The delta of the Mahakam comprises some 42 islands with a total land surface of about 1100 km² (Persoon & Simarmata, 2014). All weather and dirt roads are present only on the delta's fringe; they lead to the main villages, poor in infrastructure, and are accessible by boat only (Bosma et al., 2012). The disturbance of this ecosystem started with the introduction of a shrimp farm, and the expansion of human settlements related to the oil and gas exploration and exploitation, which attracted both workers and land speculators (Bosma et al., 2012).

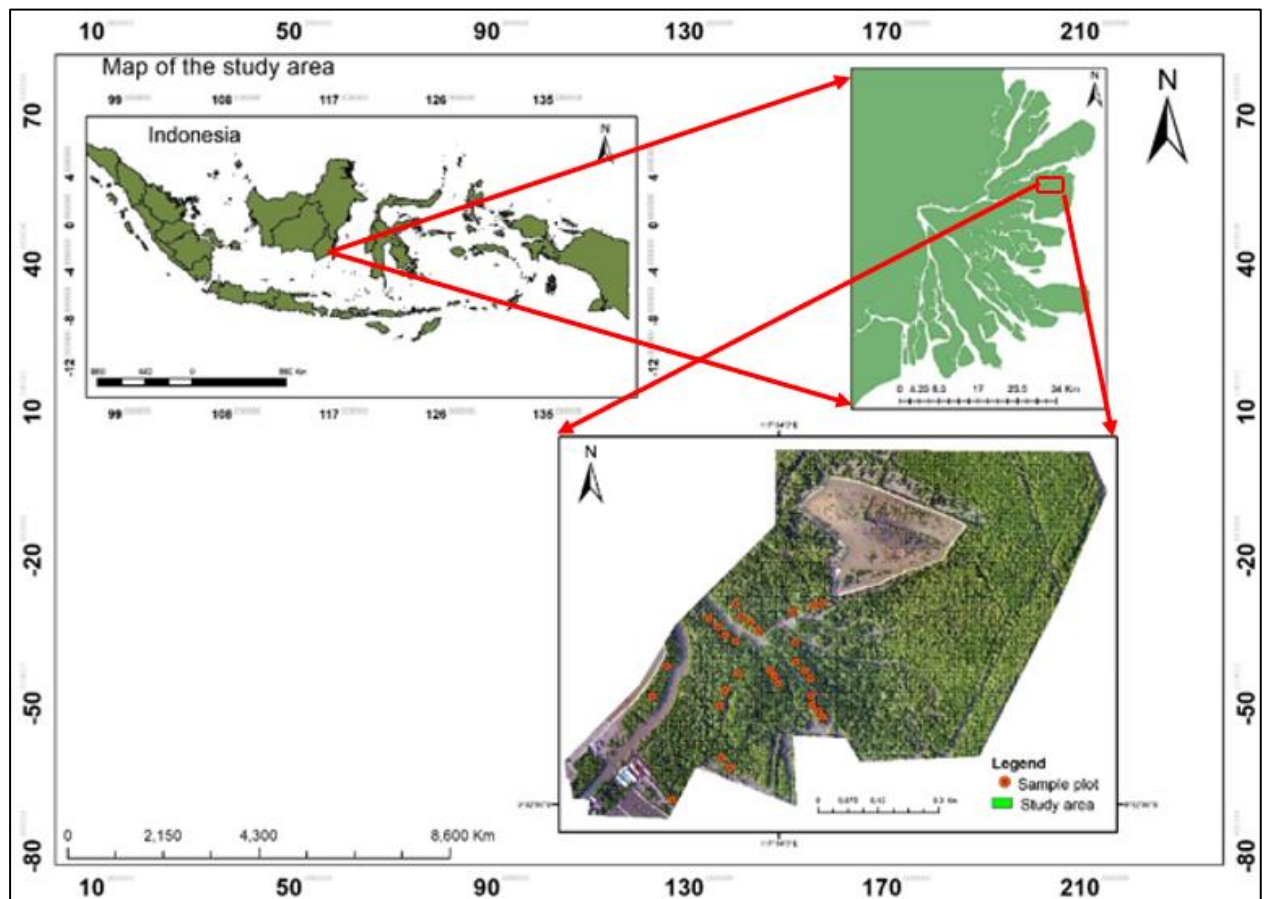


Figure 3. Map of the study area in Angan district. The overview map shows the location of the study area relative to the country (Indonesia) and Mahakam delta east coast of Borneo. The red points on the figure show the location of the plot centre.

2.1.1. Climate and Vegetation

The province of East Kalimantan is characterised by a tropical rainforest climate, with a dry condition starting from May to September and a wet from October to April, governed by the Monsoons (Persoon & Simarmata, 2014). According to Bosma et al. (2012), “The annual rainfall of the area exceeds 2,500 mm within the 25,000 km² catchment of the Mahakam river that discharges into the Makassar Strait”. The delta of Mahakam River is covered by dense mangrove, composed of mainly *Avicennia*, *Sonneratia* (*Sonneratia alba*), *Rhizophora* (*Rhizophora* spp.), and *Nypa* species (*Nypa fruticans*) and nibung (*Oncosperma* spp.); which are freshwater mangroves (Persoon & Simarmata, 2014).

2.2. Materials

Different hardware and software and field equipment used for the study during data collection and processing.

2.2.1. Field equipment

Collection of data in the field was performed using the right instruments and materials to minimise uncertainty during field data collection. Table 1 shows materials used during sample collection and the description of its functions

Table 1. Field equipment used for biometric data collection and tree scanning.

No	Instrument	Function
1	TLS (RIEGL VZ 400)	Tree scanning
2	Diameter Tape	Measure DBH
3	Clinometer	Measure slope
4	Field sheet	Record data
5	Tablet	Navigation
6	Leica DISTO D510	Measure the height
7	Handheld GPS	Take point location
8	Laminated paper	Tree labelling

2.2.2. Software

Different software was used to process and analyse the collected data from the field listed in table 2.

Table 2. Software used for data processing analysis.

No	Software	Function
1	RiSCAN PRO v2.4.2	Register and extract individual trees
2	MATLAB R2018b	Ran QSM algorithm
3	ArcGIS 10.5.1	Map generation
4	Lucid chart	Flowchart drawing
5	MS office 2010	Data analysis and thesis writing
6	Mendeley	Citation and reference

2.3. Methods

The appropriate method was designed to answer research questions, in such a way that divided into different stages which are namely; pre-field, field data collection, data processing, analysis and AGB estimation using volume derived from QSM. Pre-field activities were practical activities done to facilitate fieldwork preparation. Practising different field instruments were done such as Leica DISTO D510, GPS, Haga and Clinometer; differential GPS set up and TLS operation to collect point cloud and point cloud processing

using RISCAN PRO software. Apart from pre-field, the method used in this research comprised of four main steps. The first step was field data collection, that is a collection of tree parameters (DBH and height) in the sample plot using diameter tape and Leica. Diameter tape was used to measure the DBH of all trees with $DBH \geq 10\text{cm}$ in the sample, and Leica used for height measurement of trees. Field measured AGB/carbon stock was estimated using DBH measured by diameter tape and Height from Leica multiplied by specific and generic wood density.

The second step was data acquisition using TLS. In this stage, multiple scanning positions were used to scan all plots and generate the points cloud. RiSCAN PRO software was used to register the four scanning position sequentially using the centre scanning position as a reference. Individual trees were extracted manually to measure DBH and height of the tree using measuring tools. The DBH and height of tree derived from TLS multiplied by specific and generic wood density were used to estimate AGB/carbon stock from TLS. The third step in this research was identifying individual trees which are visible, have dense point cloud and not intermingling with others and exported as ASCII file. Then the exported tree point clouds as ASCII file was imported into MATLAB, and the data ran to generate tree volume using QSM algorithm. To estimate AGB/carbon stock of individual tree that derived from QSM tree volume generated was multiplied by wood density. The final stage in this research was to compare AGB/carbon stock that obtained from QSM and TLS with estimated from filed measured tree parameters. Figure 4 shows the flowchart of a method that has been used to address each specific objective of this study.

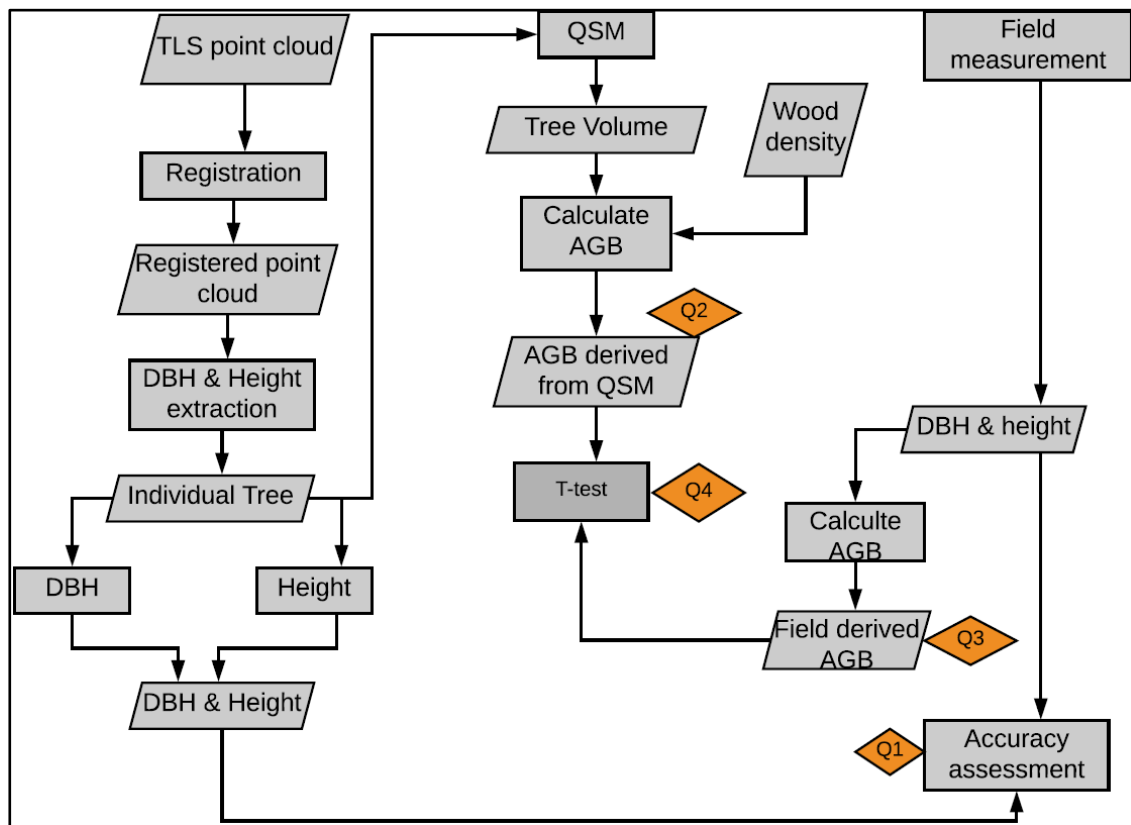


Figure 4. Flow chart of the research methods

2.3.1. Sampling Design and determination of sample plot

Mangroves are not an easily accessible ecosystem, and it is difficult to apply a random or grid sampling strategy to estimate biomass/carbon stock. By taking the study area into consideration and homogeneity of the population, purposive sampling was selected to address the research objectives. The weight of TLS, time for TLS installation in the coastal area, travel time from plot to plot and the low and high tides were also

considered to select purposive sampling. In purposive sampling, the sample chosen from the entire populations based on researcher interest and accessibility (Teddlie & Yu, 2007), but it includes all diversities. A circular sampling plot of 500m² with a radius of 12.62m was recommended for biomass/carbon estimation (Ruiz et al., 2014). The area of the sampling plot was adjusted in line with a slope of the terrain using the slope correction factor (Abegg et al., 2017). Due to the flat train of the study area, we are not using the slope correction factor to arrange the radius of our sample plot. The sample size that has greater than 600m² does not significantly improve the accuracy of the result; instead, it increases operational cost. Also, the circular plot has less error as compared to the rectangular plot (lackmann, 2011). Therefore, a circular plot of 500m² selected in which multiple scanning positions applied.

2.3.2. Terrestrial Laser Scanner plot arrangement

Before scanning started in the sample plot by TLS mounted on the tripod, numerous activities done. That enhances the laser beam from TLS to reaches the surface of a tree structure with less error (e.g., blocking or occlusion). To minimise registration error, putting the retroreflectors on visible position to the scanner is essential. Sample plot arrangement is activities done to prepare the plot for scanning. These activities are the identification of plot centre, tree tagging, placing both circular and cylindrical retroreflectors, undergrowth clearing and identifying the outer scanner positions to have full structure of the tree in all direction.

2.3.3. Centre plot identification, tree labelling and undergrowth clearing

The centre plot is the middle point in the sample plot that used as a reference to register the outer scanning position and guided where the external scanner position should install. Because of the unstable nature of the area and the mud, water, pneumatophores and aerial roots of *Rhizophora* the centre of the plot where selected on relatively stable and able to hold a tripod. By measuring a radius of 12.62m from the centre, the demarcation of the plot border done by chalk and all the trees inside the plot that had DBH of ≥ 10 cm measured and considered for AGB estimation. All the trees inside the plot that had DBH of ≥ 10 cm were labelled using laminated paper that has a number on it (Figure5).



Figure 5. Tree labelling to identify trees in the sample plot that have DBH ≥ 10 cm used for AGB/carbon stock estimation with laminated paper have a number on it attached to individual trees.

Undergrowth is bushes, shrubs and props root that block the laser beam of TLS to reach the surface of the tree. It was cleared to scan the structure of the tree in the sample plot with minimum or no occlusion and to prepare the four-scanning position of TLS one in the centre of the plot and the other three in the outer sample plot. Due to the high density of mangroves and intermingling structure of *Rhizophora* species root, this activity was time-consuming and made the work very challenging.

2.4. Terrestrial Laser Scanner data acquisition

The use of Light Detection and Ranging to estimate forest parameter started later 2000s. Similarly, the use of TLS mounted on the tripod utilises a LiDAR system which collects multiple millions of point clouds within a minute (Pfeifer et al., 2004). There are two approaches that we follow when applying TLS for point clouds data collections which performed based on the objective that we try to achieve. These two approaches are single and multiple scanning modes (Maas et al., 2008). During this study multiple scanning were performed, one at the centre of the plot and the rest (three) at different outer positions of the sample plot 2.5 m from the border of the plot (Figure 6). Total of four scanning locations within the sample plot was undertaken to get dense point cloud coverage (Thies & Spiecker, 2004). Trees within the sample plot with a DBH of ≥ 10 cm were marked to distinguish from other trees scanned with and around the sample to measure tree parameters, e.g., DBH, height, volume, etc. The point clouds which are collected from different positions in the sample plot help to get the 3D structure of the mangrove tree.

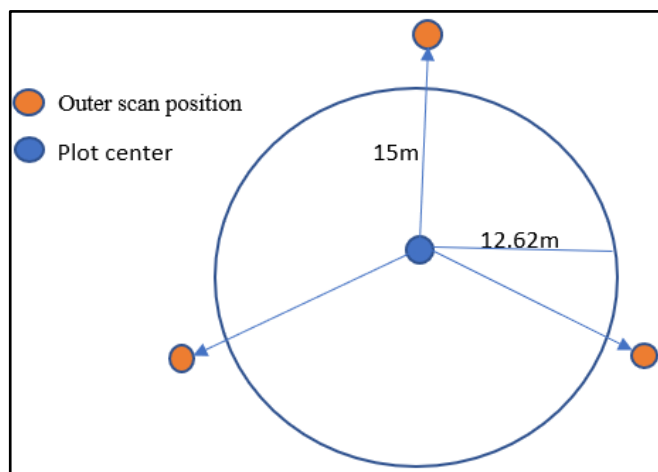


Figure 6. Multiple TLS scanning position one at the centre and the rest three approximately at 120° from each other with a radius of 12.62m. To include the tree on the border of the sample plot, it extends to 15m from the centre to edge to have dense point clouds and capture the whole structure of the tree in the sample.

2.4.1. Retroreflector

Retroreflectors are a target object used as a common point between two scanning positions to tie together as one. In multi-scanning retroreflectors are used as tie points to merge all (four) scanning position data into one single point cloud by geometric transformation using RiSCAN PRO software (Wilkes et al., 2017). Two types of retro-reflectors are used in this study; twelve cylindrical and six circular (Figure 7). When we adjusted the scanning position within the plot four cylindrical and two circular retro-reflector were placed on a place that visible to at least two scanning locations. Circular reflectors were attached to the individual tree stem, and cylindrical one was fixed on sticks distributed in the plot. However, each retro-reflectors must be visible at least between the two scanning positions and central position.

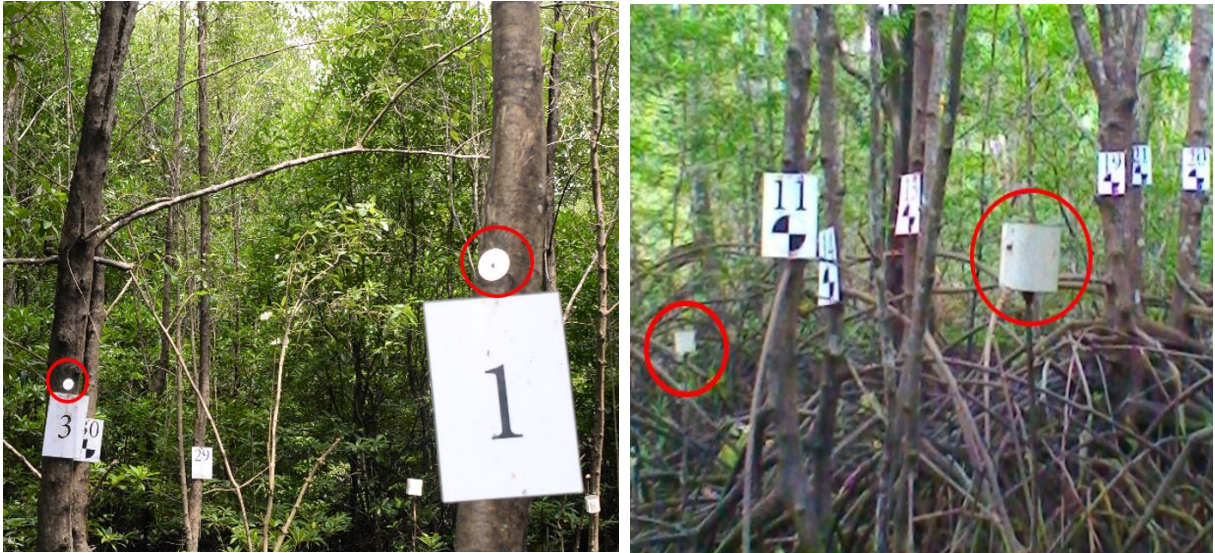


Figure 7. Both circular and cylindrical retroreflectors that used as a reference (the common point between the two-scanning position) to register all scanning position to a single data set. Circular (left) and cylindrical (right) retroreflectors used.

2.4.2. Terrestrial Laser Scanning

To capture point cloud of individual trees in the plot RIEGL VZ 400 terrestrial laser scanner was used and combined with a digital camera, a Nikon D610 mounted on the top of the TLS to obtain the actual picture of the trees. The colour pictures from the mentioned camera can be used to colour the laser point cloud of all trees in the mangrove forest. The tripod legs levelled by the guidance of position setup in the TLS. When the position of the bubble/point at the centre (Figure 8) the TLS is ready to scan, but it is very challenging and time-consuming in mangrove forests to fix the point to the centre. The setting of TLS that we used to acquire dense point clouds of tree structure indicated in table 3.

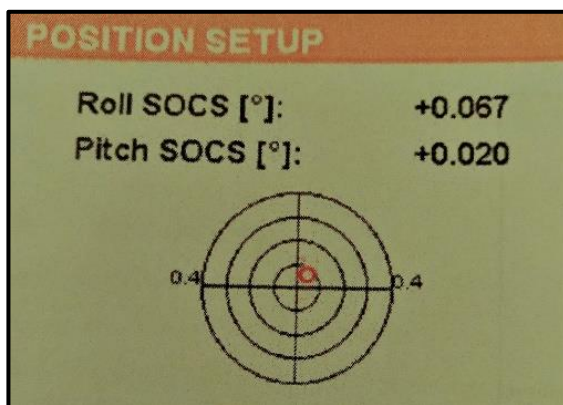


Figure 8. TLS Levelling setup that accurately scans the surface of the trees with a small error

Table 3. TLS scanner setting used during the field work.

No.	Parameter	Setting
1	Minimum range	1.5m
2	Reflector diameter	0.10
3	Reflectance threshold	0.10
4	Image acquisition	ON
5	Reflector search	ON
6	Register reflector auto	ON
7	Registration Mode	Reflector local
8	Scan Mode	Panorama 40

2.5. Biometric data collection

Field data collection in the study area was performed from September 26 to October 28, 2018. Mangrove trees that have a DBH of \geq to 10 cm within the sample plot were measured and considered for biomass/carbon stock estimation. The contribution of a tree that has less than 10 cm diameter is insignificant to the biomass/carbon stock (Brown, 2002). DBH is a diameter at 1.3 m above the ground. However, in this study, we follow two to approach to measure DBH of the tree based on the species. In the case of *Rhizophora* species we measured DBH at 0.2 to 0.3 m from the top of prop root (Figure 9), but for *Avicennia*, DBH measured at 1.3 m from the ground as *Avicennia* does not have prop root. A stick having 1.3 m height was used in the field for consistent measurements. A tree that has a fork below 1.3 m were considered as two different trees, but that have above 1.3m was recognised as one, and the tree height was measured using Leica DISTO D510.



Figure 9. *Rhizophora* species that need to climb them to measure DBH in the field using diameter tape.

2.6. Pre-processing of point cloud

After data acquisition done in the field, pre-processing of acquired data followed to process and analyse the data. Pre-processing activities started by registering the multiple scanning positions in each sample plot. During registration performed all the scanning positions (four) combined into one single point with the help of tie points distributed in the field uniformly using dedicated programmes (Dassot et al., 2011). RiSCAN PRO v2.4.2 software was used to register and merge all the scanning positions sequentially using the centre scanning position as a reference. When all scanning positions successfully registered single tree extraction is the next step and time-consuming processes.

2.6.1. Scanning position registration

The multiple scanning positions which performed in this study was registered by exporting the scanned data from TLS to fish disk and imported to the computer to start pre-processing in RiSCAN PRO software. To introduce all scanned locations to RiSCAN PRO, we start a new project under the project menu and by using the help menu as indicated in figure 10. All the scan positions automatically registered by using the centre scanning position as a reference with the help of common reference point using retroreflectors, which are managed by Tie point List (TPL) (RIEGL, 2014).

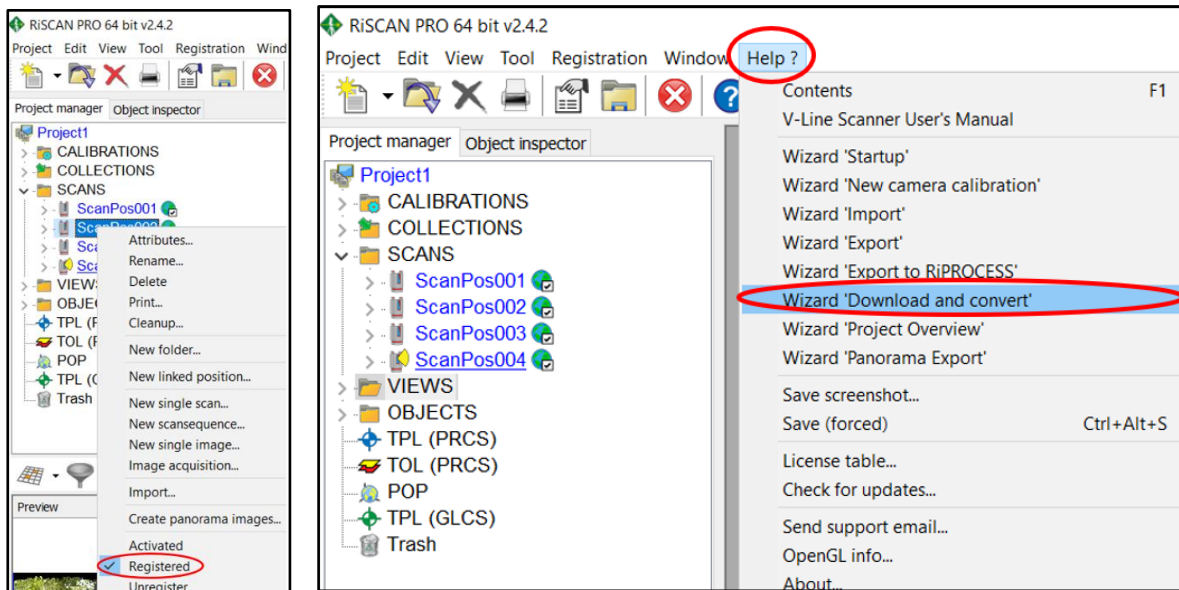


Figure 10. The procedure that shows how to register the different scanning positions using the centre scanning as a reference on RiSCAN PRO software.

2.6.2. Extraction of individual tree

Individual trees were extracted from registered Terrestrial Laser Scanner point clouds manually using RiSCAN PRO software. Three hundred fifty trees which have dense point cloud, clearly visible to the laser beams not intermingling with other trees extracted from 30 plots. TLS data processing could comprise multiple scans, background vegetation, and non-related vegetation which filtered out until the point clouds of individual trees obtained. After the registration of pint clouds of all four scanning positions, individual trees were extracted manually to measure DBH and height using measuring tool in RiSCAN PRO (Figure 11). The biomass of single tree estimated by allometric equations and compared with biomass that derived from TLS and QSM.

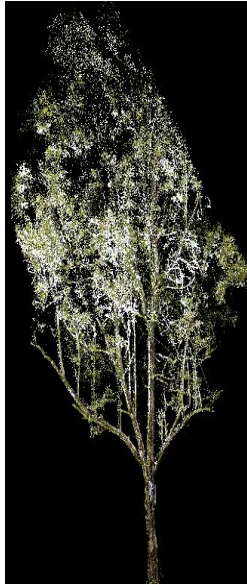


Figure 11. Manually extracted individual tree with true-colour and saved as poly data for further analysis.

2.7. Tree parameters extraction and measurement

Individual tree DBH and height measured from a manually extracted tree in RiSCAN PRO software using measuring tools. The extracted tree saved as ploy data after removing noise (i.e., point clouds that is not part of the tree or from the nearby tree) and branches and canopy of another surrounding or overlapping trees. Two different approaches were used to measure DBH of the trees depending on the species of mangroves. Commonly *Avicennia* and *Rhizophora* are the two species in the study area. *Rhizophora* species have prop root to cope up with the high tide and aeration they rise their root above the ground; in some cases, it goes up to 2 m (Figure 9). As a result, DBH measurement of *Rhizophora* spp. was measured from the end of the upper prop root 20-30 cm (Kangkuso et al., 2018) but in *Avicennia* spp., it starts from the ground, and we have used 1.3m above the ground to measure DBH (Figure 12). The height of the trees also measured by using the highest and lowest two points from the point clouds of the individual tree using the measuring tools in RiSCAN PRO software. Figure 13 shows the tree extracted and how its height was measured.



Figure 12. Individual tree DBH measured from manually extracted point clouds using measuring tools in RiSCAN PRO software.



Figure 13. Individual tree height measured from extracted point clouds found in the upper and lower part. Which means the difference between the two-point cloud gives the height of the tree.

2.8. Conversion of point clouds into ASCII format and QSM

The extracted individual trees point cloud converted and exported as an ASCII text file, that is a readable file format in MATLAB software. All individual trees data were exported and changed to x, y, z which makes it ready for 3D tree structure construction using the export function in RiSCAN PRO software. Reconstruction of the individual tree using QSM, done after TLS point clouds of each tree were exported as an ASCII and imported/loaded to MATLAB (R 2018b) software. The procedural step that was taken during we performed tree QSM in MATLAB listed in the following sub-sections.

2.8.1. Filtering of point clouds

Filtering is the method in which we try to remove unwanted points which are not part of the tree. It takes place two times before and during QSM construction (Akerblom, 2012). When filtering performed appropriately, some points in the point cloud which are not part of the tree structure, and consequently noise minimised, this would improve accuracy and computations time Raumonon (2015). In the step of reconstruction of the individual tree using QSM, point cloud which is not a part of the wooden structure and point cloud from the nearby tree must remove before running the algorithm in MATLAB for the process of reconstruction. Filtering which performed during the pre-processing removes the points that far away from the tree, while initial screening removes point cloud which does not involve in the structure of the tree. The final filtering stage removes the noise point cloud generated during the scanning process by TLS it self (Akerblom, 2012). A cover set removes point cloud which is not part of the tree (Raumonon et al., 2013). Raumonon et al. (2013) stated that the size of the cover set depends on the density of the individual tree point cloud. Figure 14 showed an excellent example of an extracted tree with (205927) and filtered (151920 points) tree left to right. The filtering command that we used to perform filtering on Matlab described in the following.

Pass = filtering (P0, r1, n1, d2, r2, n2, Scaling, Comp);

P = P0 (Pass, :);

Where,

P0	Unfiltered point cloud.
r1	Radius of the ball used in the first filtering.
n1	Minimum number of points in the accepted balls of the first filtering.
d2	Minimum distance between the centres of the ball in the second filtering.
r2	Radius of the ball used in the second filtering.
n2	Minimum number of the ball in the components passing the second filtering.

Optimal inputs, default value false:

Scaling If true, the first filtering threshold “n1” is called along the height with an average point density

Comp If true, does the first filtering process for every point.

The unit of radii (r1 and r2) and distance (d2) are in a meter. When we run the filtering with the same parameters, it generates different cover set which randomly generated (Raumonen et al., 2013).

r1= smallest size of the beaches to be modelled (Akerblom, 2012) 0.015 m to 0.25 m used in this study.

d2= the recommended value is approximately 0.01 to 0.03 m (Raumonen et al., 2013).

r2= r2 greater than d2. it is recommended that r2 should be higher than d2 by half or a centimetre (Raumonen et al., 2013).

You are scaling and Comp= 1 if true or 0 if false.

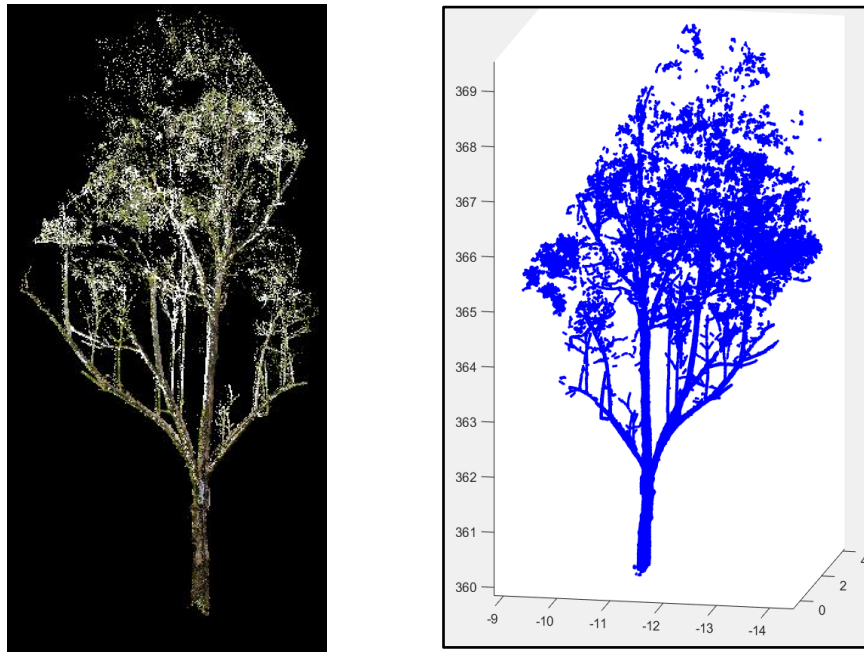


Figure 14. Extracted individual tree before filtering (205927 points) (left) and after filtered (151920 points) (right)

2.8.2. Optimisation of input parameters in QSM

The following show how QSM algorithm optimise the input parameters when TLS point clouds represent or reconstruct a tree.

QSM tree (P, PatchDiam 1, BallRad1, nmin1, PatchDiam2Min, PatchDiam2Max, BallRad2, nmin2, lcy1, OnlyTree, Tria, string, FilRad);

where:

P	(Filtered) point cloud, (m_points x 3)-matrix, the rows give the coordinates of the points.
PatchDiam1	Cover set the size of the first uniform size cover.
BallRad1	Ball size used for the first cover generation.
Nmin1	Minimum number of points in BallRad1-balls.
PatchDiam2Min	Minimum patch size of the cover sets in the second cover.
PatchDiam2Max	Maximum cover set size in the base of the stem in the second cover.
BallRad2	Maximum ball size used for the second cover generation.
Nmin2	Minimum number of points in BallRad2-balls.
Lcy1	Cylinder length/radius ratio. Can have multiple values, in which case makes as models with the same segmentation.
OnlyTree	Logical value, true if only points from the tree to be modelled, in which case defines the base of the trunk as the lowest part of the point cloud.
Tria	Logical value, if true, then make triangulation for the stem up to the first branch.
String	Name string for saving output files.
FilRad	Optional input, the relative radius for outlier point filtering. Can have multiple values in each case make as many models with the same segmentation.

The rules of thumb while performing reconstruction of the individual trees are mentioned in the following paragraph.

The value of BallRad1 and BallRad2 should have higher than PatchDiam1 and PatchDiam2max, $BallRad2 = PatchDiam2max + 0.01$ (Raumonen et al., 2013). To ensure that the cover set next to each other and intersect BallRad should be more prominent (Raumonen et al., 2013). 0.14 m and 0.13 m are the value that used for BallRad1 and BallRad2 respectively during this study.

PatchDiam1 and BallRad 1 value are not very important, but comparatively, it should be greater than PatchDiam2Min. As Raumonen et al. (2013) have indicated, the value for PatchDiam1 ranges between 8 cm to 16 cm and consequently, the first segmentation used to remove the points that do not belong to the tree structure and to remove this point cloud PatchDiam1 and ballRad1 values used. In this study, 0.12 m used as a value for PatchDiam1.

The patchdiam2min value should be close to the value of the smallest branch to be modelled (Akerblom, 2012). As Raumonen et al. (2013) have indicated PatchDiam2Min parameter governs the size of the cover set which ultimately affects the QSM result. The value for PatchDiam2Min varies based on the individual tree to model. During this study, we used the value that ranges from 0.01 to 0.03 m to perform the reconstruction process.

Lcyl controls the average relative length of the cylinders. Lcyl and the size of the cylinder has a direct relationship, the bigger the Lcyl, the longer the fitted cylinder (Raumonen et al., 2013). When the cylinder is shorter, it is better to model the local diameter of the branches, but the direction can be varied and noisy. Consequently, the diameter may be too large or too small (Raumonen et al., 2013). The value that used for Lcyl in this study is 3 and 3.5.

FilRad defines the relative radius for outlier point filtering before least square fitting (Raumonen et al., 2013). By using 3.5 as the default value for FilRad, the point which is farther than 3.5 times the estimated radius are filtered from the region (Raumonen et al., 2013). This default value may vary depending on the noise and co-registration accuracy which minimises the effect of the default value. Apart 3.5 default value of 1.5 and 2.5 that ensure the fitted cylinder is not too big (Raumonen et al., 2013). The value 1.5 and 3 were used as FilRad value in this study depend on the point cloud of the individual tree to model.

Nmin is the minimum points in a cover set. Calders et al. (2015).stated that the value sets the threshold if a cover is kept or discarded in the reconstruction process and it is robust to a certain threshold. It leads to overestimation or underestimation of constructed volume (Calders et al., 2015).

Optimum selection of input parameter is very critical to run QSM algorithm. Reconstruction quality of individuals tree depends on the careful selection of the parameters. The optimum modelling parameter which significantly crucial in the reconstruction processes are PatchDiam2Min, Lcyl, and FillRad. However, PatchDiam2Min is the most important compared to others. Figure 15 shows the wooden tree structure using the TLS point cloud and QSM.

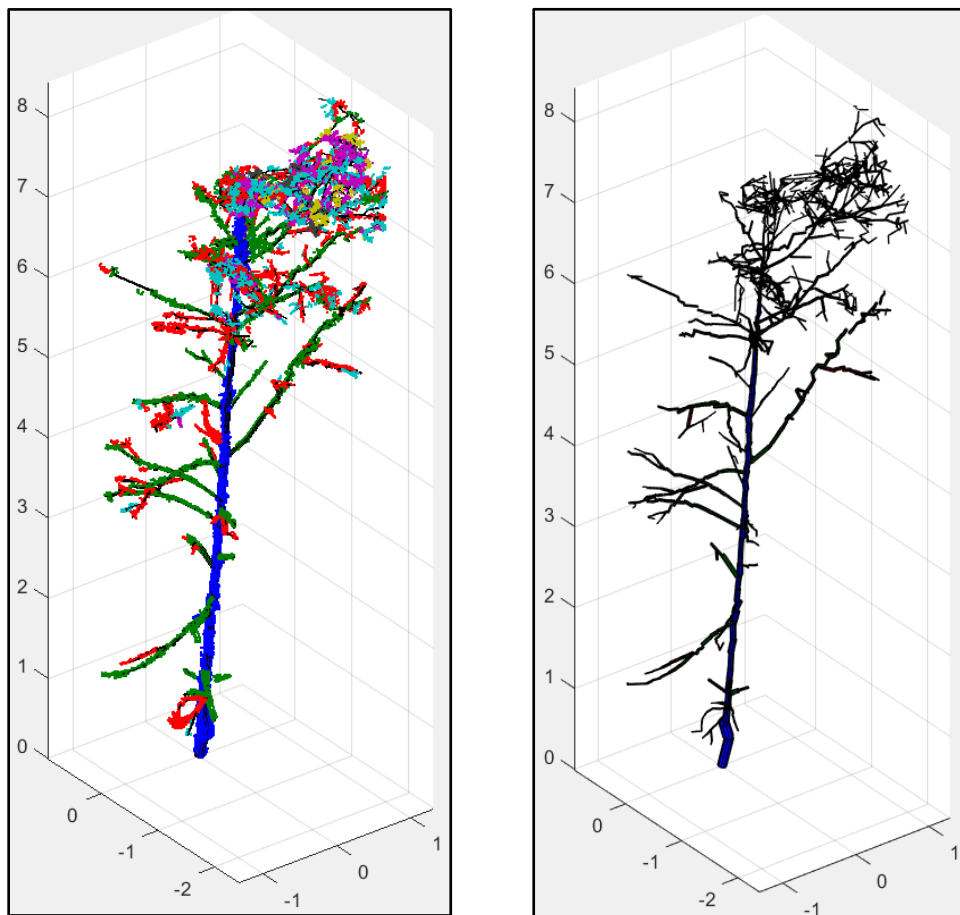


Figure 15. A segmented tree structure with a different colour (left) and the segmented structure fitted to the cylinder to estimate the volume of a tree to (right).

2.8.3. Steps of the reconstruction process.

Figure 16 shows the main steps in the reconstruction process of individual tree in MATLAB using the QSM algorithm. The flow chart in figure 16 and subsections describe the procedure followed in the reconstruction of the individual tree to generate volume in detail.

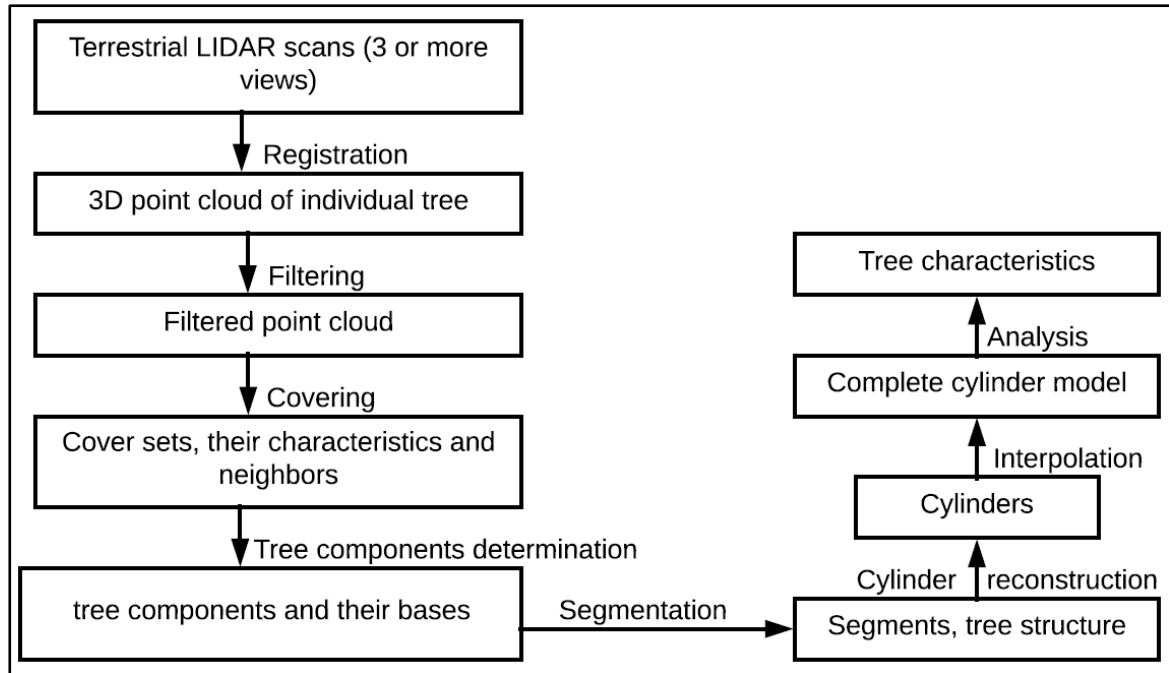


Figure 16. Main steps of reconstruction a tree using QSM (Raumonen et al., 2013)

2.8.4. Cover sets.

Cover sets is a spherical centre of the point with radius r (Akerblom, 2012). If the point cloud is P , then the cover set is a subset of P , and the union of all the cover set is a complete point cloud which follows the principle of set theory (Akerblom, 2012). When we run QSM for reconstruction of an individual tree, we use a cover set approach which partitioned point cloud into small sets that correspond to small patches on the surface of the tree (Raumonen, 2017). Cover sets are like building blocks that one on top of the other to form the whole tree structure from the bottom to top (Calders et al., 2015). It generated by spherical neighbourhoods of randomly selected points from the point cloud with the help of input parameters, and it differs from iteration to iteration (Akerblom, 2012). Diameter (d) and radius (r) which is the minimum distance between the centres of two balls and radius of the spherical ball respectively determine cover sets (Raumonen et al., 2013). The size of the cover set radius chosen by considering the size of the individual scanned tree that needs an understanding of the scanned tree before running the algorithm (Akerblom, 2012). The two-extreme size of the cover set (whether it is too big or too small) leads to overestimation or underestimation (Raumonen et al., 2013) (Figure 17). The rule of thumb for tree reconstruction is the radius of the cover set should be equal to the smallest branch size to be modelled (Akerblom, 2012) and the diameter (d) should be smaller or equal to the radius (r) (Raumonen et al., 2013). The intersection of one BallRad with other BallRad of cover set form neighbour relation (Raumonen, 2017). Due to these intersection points belong to multiple balls, but the ball which is far from the centre of the ball assigned to the nearest ball (Akerblom, 2012).

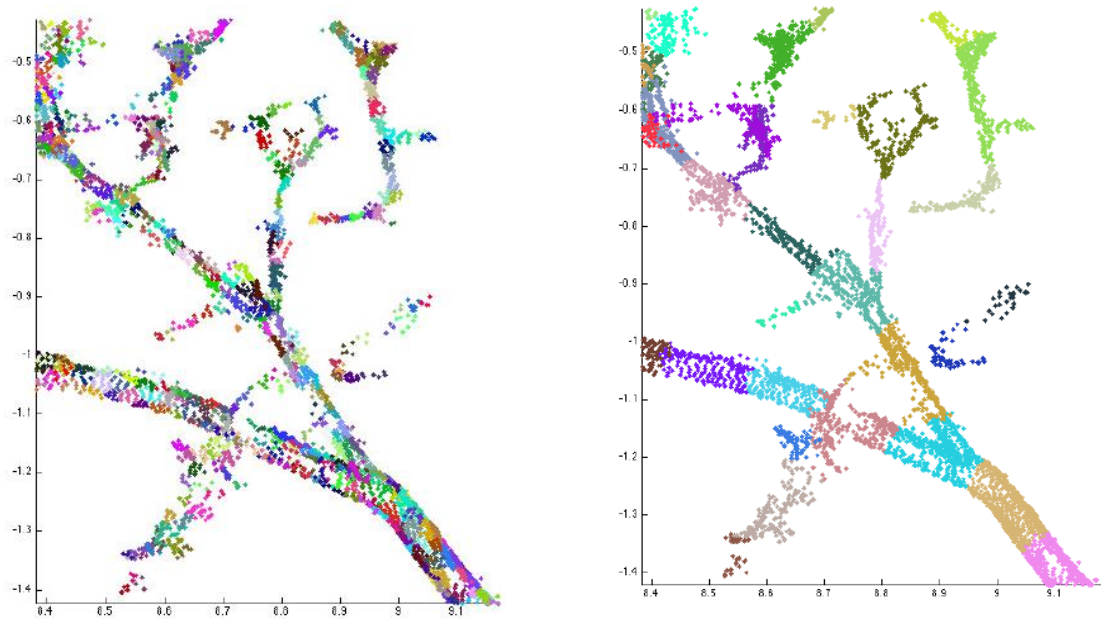


Figure 17. Minimum cover set 2 cm (left) and maximum cover set 10 cm (right) (Raumonen et al., 2013).

2.8.5. Tree Components

After cover set generation, determination of neighbour relation and geometric characteristics of a set, extracting the cover sets that about the tree is the next step (Raumonen et al., 2013). To define the base of the trunk, the point cloud which is not part of the tree and that contain ground must first be removed (Raumonen et al., 2013). In this step reconstruction of tree start from a single component from the base upwards. Therefore, a maximum set of connected cover sets defined as a component (Akerblom, 2012). To come up with tree component first trunk is described as a set of cover sets that are parallel to the trunk direction and redefined trunk by including its neighbouring cover set (Raumonen et al., 2013).

2.8.6. Segmentation

The component is a base for segmentation. After tree components and the determination of its base segmenting those components into branches is the next step (Raumonen et al., 2013). Components are partitioned into segments that match to the whole or part of the branch or trunk (Raumonen et al., 2013). The segmentation process based on the topology of the individual tree (Akerblom, 2012). The relation of a tree structure is a child and parent branch relation for each branch that is described by segmentation (Raumonen et al., 2013). While segmented branches separated from the stem and the base of the branch defined, the process continue until possible bifurcation is determined (Akerblom, 2012). The sequence of segmentation starts from the base, first-order branch, second-order branch, etc. until the whole individual tree is segmented (Raumonen et al., 2013).

2.8.7. Cylinder reconstruction

By approximating the radius and orientation of the segment, the cylinder is fitted to the section using the least square fitting method (Akerblom, 2012). L_{cyl} controls are the average length of the cylinder, the bigger the L_{cyl} , the longer the fitted cylinder and the shorter L_{cyl} , the smaller the cylinder which is better to model the diameter of the branches (Raumonen et al., 2013). Unrealistic cylinder reduced by checking the radius of parent and child segments. To control the variation, the radius of the child branch should be smaller than the parent branch (Akerblom, 2012).

2.8.8. Completing the cylinder model

To assure that when segment reconstructed with a cylinder, the segment should connect each other continuously which means that there is no gap between each cylinder (Raumonen et al., 2013). As a result, the statistical error reduced by closing the hole between the parent and child cylinder through refined the cylinder model and the opening between the cylinders closed by a previously fitted cylinder (Raumonen et al., 2013). The green cylinder has no extension, and the nearby blue cylinder has no parent. The gap between these two cylinders filled by the red cylinder (Figure 18).

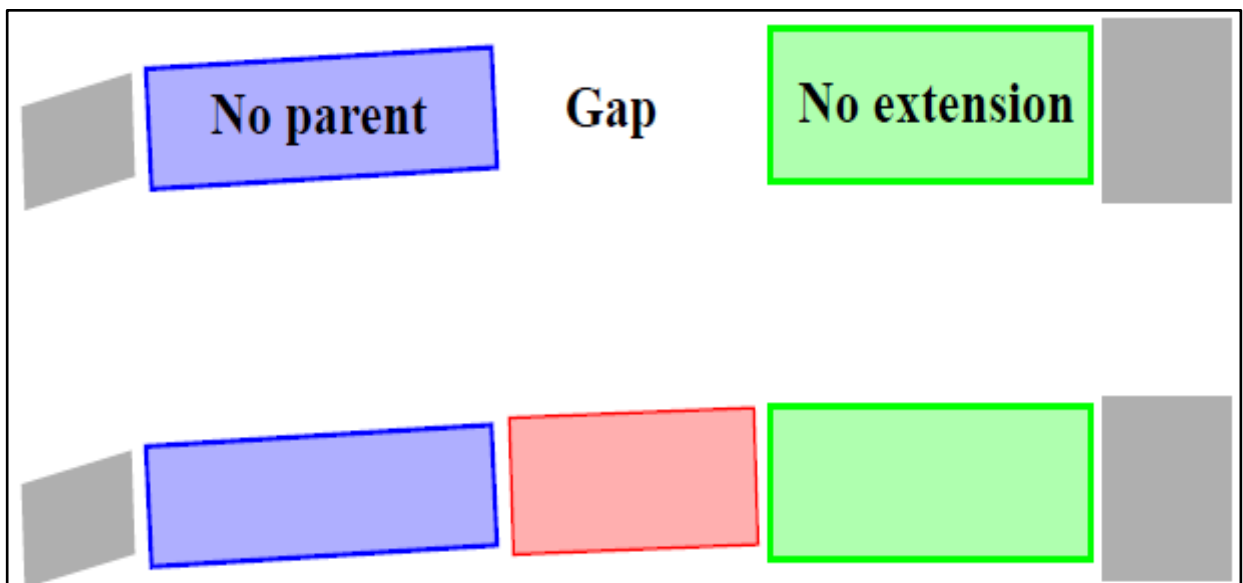


Figure 18. Filling gap to reconstruct the whole structure of a tree (Raumonen et al., 2013).

2.8.9. Tree characteristics

When we ran a single tree point cloud in MATLAB using QSM algorithm tree characteristic generated are total tree volume (the sum of trunk and branch volume), tree height, DBH, branch order and a total number of the branches. Total tree volume obtained from QSM multiplied by wood density to assess AGB/carbon stock of a single tree. Finally, AGB assessment by TLS using QSM done for the individual tree.

3. RESULT

3.1. Descriptive Statistics

Using SPSS software and Microsoft excel, descriptive statistics were carried out on DBH and height derived from TLS and measured in the field using diameter tape and Leica DISTO laser Ranger. A tree which has dense point cloud and not intermingling with the nearby tree was selected to perform DBH and height measurement from the sample plot. A total of 350 trees were manually extracted from each sample plot of TLS point cloud using RiSCAN Pro. Thus, for each one of the extracted trees, DBH and height were measured and compared with field-measured tree height and DBH using Leica and diameter tape respectively (Figure 17). To provide information about the tree structure and biomass, DBH is the most critical tree parameter (Zulkarnain et al., 2017). Details of DBH and height measured by both methods (i.e., field and TLS) described in the following section.

3.1.1. Diameter at Breast Height (DBH) measurement

A descriptive statistic was conducted to observe the relation between the mean and standard deviation of field measured DBH (mean=15.19, Std.Dev.=5.57) and TLS derived DBH (mean= 15.08, Std.Dev.=5.47) (Appendix 3). These results suggest that DBH measurement in the field using diameter tape and derived from TLS point clouds using measuring tools in RiSCAN PRO software were highly correlated.

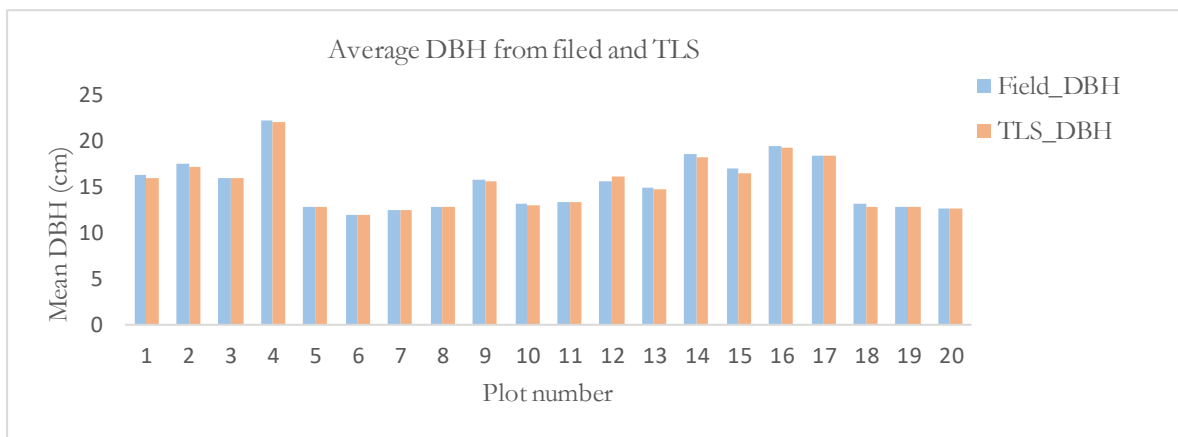


Figure 19. Field measured DBH (blue) with average 15.19 cm, and TLS derived DBH (orange) with an average value of 15.08 cm. Plot number 2, 4, 14, 16 and 17 has remaining old trees; the rest plots are similar, and all young plantation.

3.1.2. Height measurement

The relationship between tree height measured in the field using Lecia and tree height derived from TLS indicated using descriptive statistic. The mean and standard deviation measured by Lecia was (mean=13.33, Std.Dev=2.63) and that of TLS was (mean=12.76, Std.Dev=2.71). Even though it is difficult to measure tree height in tropical rainforest using a handheld lesser and TLS, however, the results of this study suggest that tree height measurement by using both technics does not show significant difference due to the young and open canopy of mangrove forest in this study area.

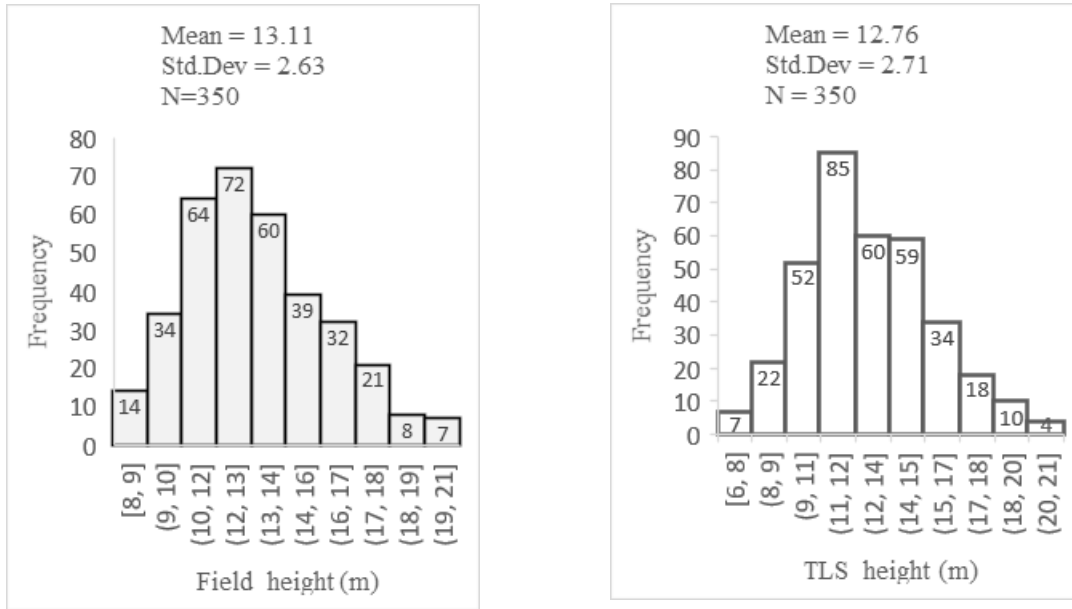


Figure 20. Distribution of field measured tree height (left) and TLS derived height (right).

3.1.3. Mangrove forest tree species

The two-dominant mangroves trees species in the study area are *Rhizophora* and *Avicennia*, and the percentage of each species described in figure 20.

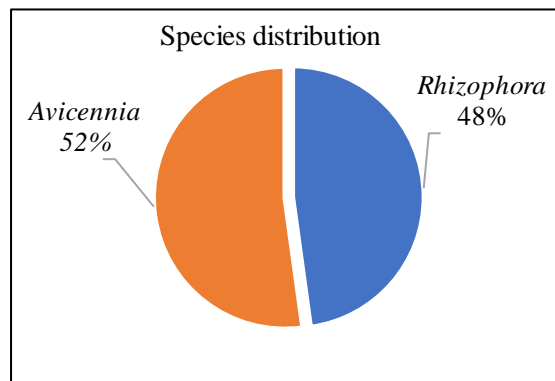


Figure 21. The dominant mangrove tree species in the area

3.2. The relationship between TLS derived, and field measured DBH and height

The estimated DBH and height derived from TLS and field measurement (Figure 21 & 22) show a strong relationship. The two figures showed a very high correlation between the two methods with a coefficient of determination (R^2) 0.978 with RMSE of 0.62 cm for DBH, while a reasonable R^2 0.73 with RMSE of 1.93m for height were found between the TLS and field measured. The relation between the two methods was confirmed using a t-test performed at a confidence interval of 95% ($\alpha = 0.05$). These results suggest that there is no significant difference between DBH derived from TLS and DBH that measured in the field using diameter tape (Appendix 10).

Similarly, there is no significant difference between height measured by Leica and derived from TLS point clouds (Appendix 10). As a result, the null hypothesis that stated, there is no significant difference between the two methods was accepted at a 95 % confidence interval. See Appendix 9 for the details t-test of the substantial difference between TLS and field measured DBH and height.

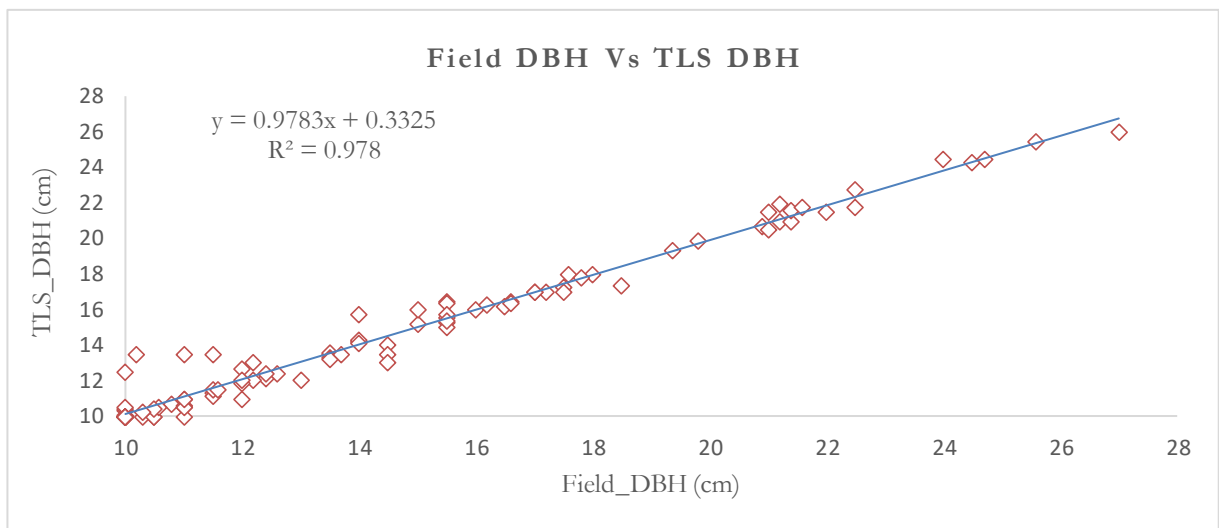


Figure 22. The relationship between field measured, and TLS derived DBH which shows a high correlation of R^2 0.978 with RMSE of 0.62 cm.

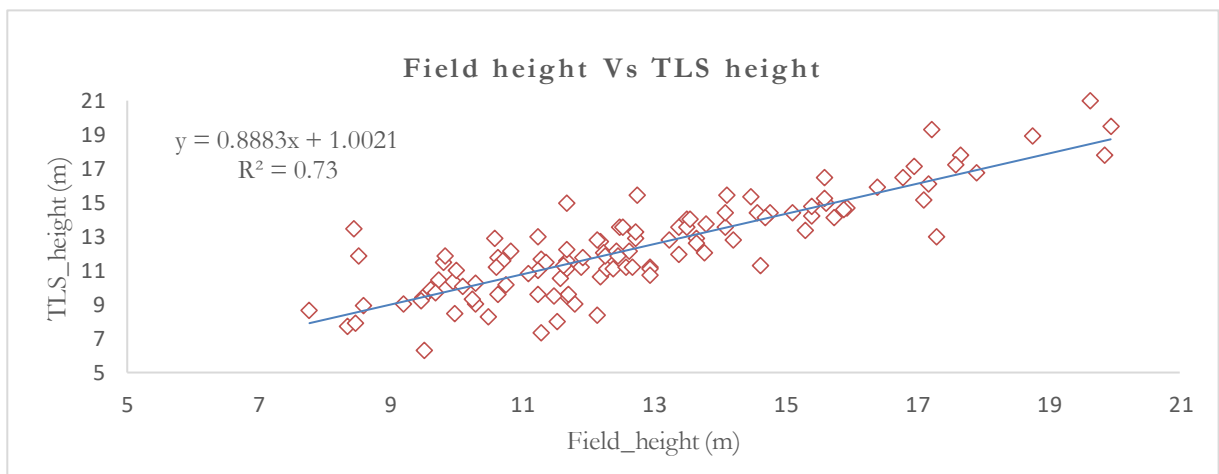


Figure 23. The relationship between field-measured and TLS derived tree height which indicates there is no significant difference between the two methods with R^2 0.73 and RMSE of 1.92 m

3.3. The relationship between TLS obtained, and field measured DBH and height

3.3.1. Above ground biomass estimated using field-measured tree parameters

Estimation of AGB/carbon stock using field measurement requires allometric equations that shows the amount of AGB/carbon stock stored per individual tree. To estimate ABG/carbon stock of the study area the allometric equations from Chave et al. (2005) was applied $(0.0673 * (\rho * D^2 * H)^{0.976})$ using general and specific wood density depending on the type of species by global wood density. The AGB/carbon stock of each tree calculated which was used as a reference to assess the accuracy of AGB/carbon stock that derived from TLS and QSM. One hundred fifteen (115) trees were selected to be used to estimate biomass/carbon stock using TLS and QSM. Table 4 indicates the descriptive statistics of the above-ground biomass estimated using generic (M=94.59) and specific wood density (M=11.86) multiplied by DBH and tree height measured in the field. These results indicate that when we used species-specific wood density the mean AGB per tree increased by 19 %, but statistically, there is no significant difference between species-specific and general wood density in estimating AGB/carbon stock (Appendix 5).

Table 4. Descriptive statistics of above ground biomass from field measured using generic and specific wood density.

<i>Field_AGB descriptive statistics (default)</i>		<i>Field_AGB descriptive statistics (SWD)</i>	
Mean	94.59	Mean	116.86
Standard Error	7.13	Standard Error	9.05
Median	61.09	Median	76.55
Mode	37.12	Mode	50.70
Standard Deviation	76.09	Standard Deviation	96.64
Sample Variance	5789.68	Sample Variance	9338.44
Kurtosis	2.53	Kurtosis	3.41
Skewness	1.64	Skewness	1.80
Range	358.07	Range	498.86
Minimum	25.80	Minimum	30.30
Maximum	383.88	Maximum	529.16
Sum	10783.82	Sum	13322.25
Count	115	Count	115
Confidence Level(95.0%)	14.119	Confidence Level(95.0%)	17.93

3.3.2. Above ground biomass derived from TLS point clouds

Above-ground biomass derived from TLS estimated from point cloud data with the help of RiSCAN PRO software, DBH and height of a tree measured. The general and specific wood density were used to estimate AGB/carbon stock by Chave et al. (2005) allometric equation (Appendix 5). The statistical data about AGB derived from TLS using general and specific wood density shows there was an increment in mean AGB by 18.99 % when specific wood density was used. However, the overall result shows there is no significant difference between general and specific wood density to estimate AGB/carbon stock (Appendix 5).

3.3.3. The relationship between AGB derived from TLS and field-measured tree parameters

The estimated AGB in both general and specific wood density using allometric equations does not show a significant difference between AGB derived from TLS estimated tree parameters and from field measured tree parameters. Figure 23 & 24 shows the relation between AGB derived from TLS and field measured with the coefficient of determination R^2 0.978 and RMSE of 14.49 kg/tree for specific wood density and R^2 0.978 with RMSE of 11.41 kg/tee using generic wood density. These results suggest that estimation of AGB in both methods are highly correlated.

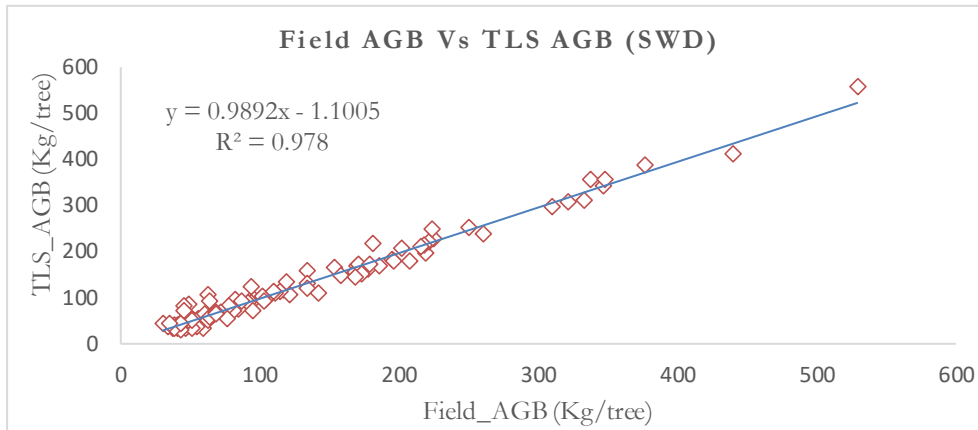


Figure 24. The relationship between field-measured AGB and TLS derived AGB using specific wood density show high correlation $R^2=0.978$ and RMSE 14.49 kg/tree.

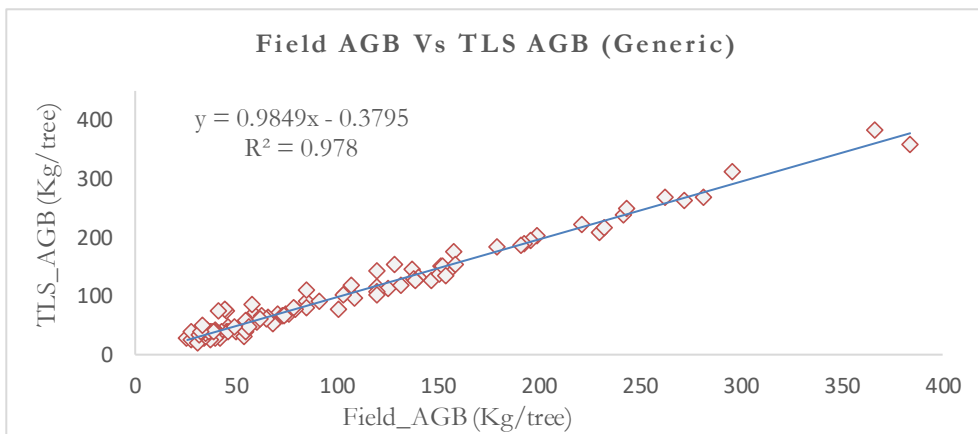


Figure 25. AGB derived from TLS was highly correlated with field measured AGB with R^2 0.978 and RMSE of 11.41 kg/tree which reject alternative hypothesis by accepting the null hypothesis at 95% degree of the confidence interval.

3.3.4. Testing the relationship between AGB derived from TLS and field-measured tree parameters

The significant difference between above ground biomass/carbon stock from TLS and field measured was tested using t-test assuming equal variance. The result suggests there was no significant difference in the AGB estimated from field measured tree parameters using specific wood density ($M=116.86$) and AGB derived from TLS ($M=114.5$) (Appendix 11).

Similarly, there is no significant difference between AGB estimated from field measured tree parameters using generic wood density ($M=94.59$), and AGB estimated from TLS derived tree parameters ($M=92.79$) (Appendix 11). However, there is an increment of AGB kg/tree using specific wood density, but it is not statistically different when generic wood density applied. As a result, the alternative hypothesis nullified, and the null hypothesis which dictates there is no significant difference between the AGB derived from TLS and field-measured tree parameters was accepted.

3.3.5. Above ground biomass derived from QSM

A quantitative structural model algorithm is implemented to generate different tree parameters; among those parameters, total tree volume is essential to estimate above ground biomass/carbon stock of an individual tree. As Raunonen et al. (2013) indicated, the output of the QSM model differs in a different run using the same input parameter. Therefore, to cope up the errors generated during processing and to get a relatively accurate measurement, the QSM model ran five times. The tree volume estimates were produced by taking the average of these five ran. Out of 350 trees extracted 115 trees which are visible, have dense point cloud

and not intermingling with others are selected for QSM reconstruction. The result presented on appendix 13 shows descriptive statistics of AGB derived from QSM using both general and specific wood density. The average AGB estimated by multiplying tree volume with specific wood density is greater by 26.2% than that obtained by generic wood density. These results suggest that there was a significant difference in the AGB estimated using specific wood density (M=122.92, SD=104.06) and AGB assessed using generic wood density (M=90.76, SD=76.75). Details of statistical data that show the significant difference of specific wood density indicated in appendix 7.

3.3.6. The Relationship between AGB derived from QSM and field measured AGB

The relation between above ground biomass derived from QSM and AGB from the field using allometric equation resulted in R^2 of 0.9638 with RMSE of 15.05 kg/tree for general wood density and R^2 0.965 with RMSE of 21.08 kg/tree for specific wood density (SWD). Figure 25 & 26 show the relation between AGB derived from QSM and field measurements using specific and generic wood density respectively. These results suggest that estimation of AGB using specific and generic wood density multiplied by field-measured tree parameters and tree volume derived from QSM shows there is no significant difference. Specifically, the result suggests that when specific wood density used, there are high correlations between AGB from QSM and field-measured AGB using specific wood density.

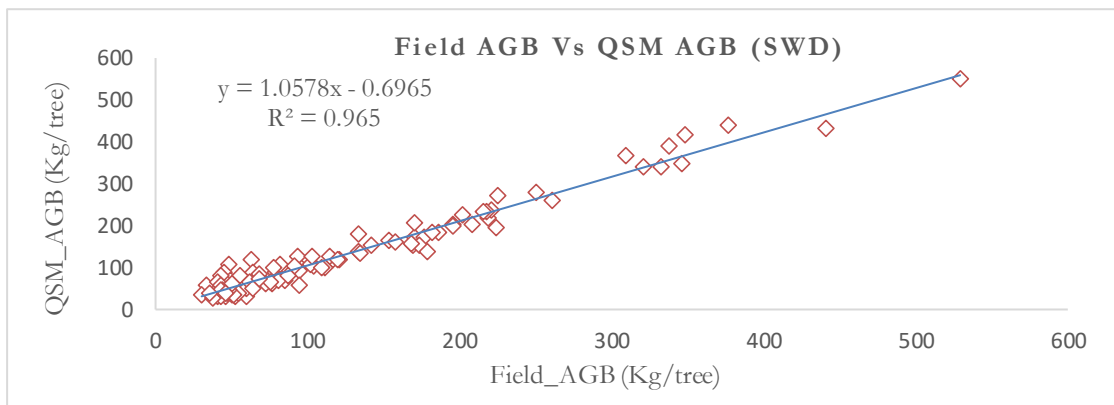


Figure 26. The AGB derived from QSM highly correlated with the reference field measured AGB using specific wood density. The result show AGB derived from TLS using QSM is accurate.

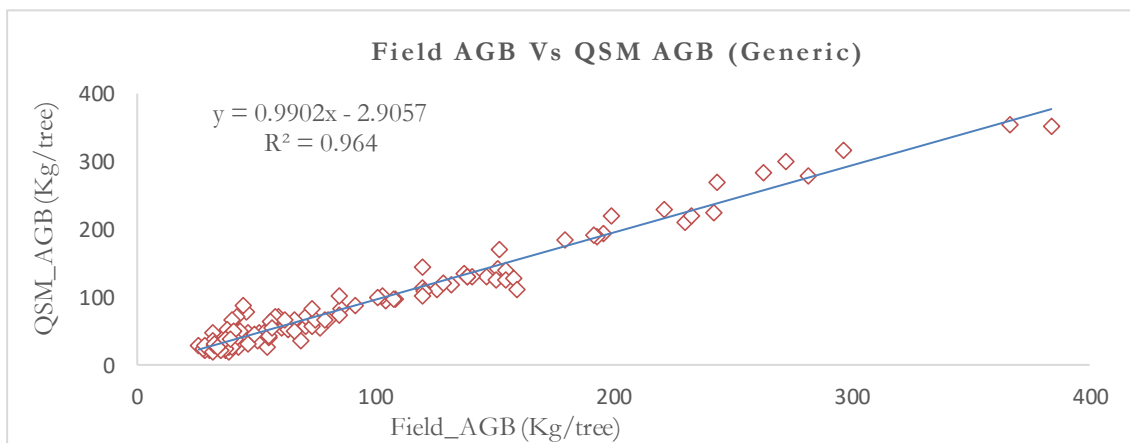


Figure 27. Above ground biomass derived from QSM using generic wood density is highly correlated with ABG estimated from field measured.

3.3.7. Testing the Relationship between AGB derived from QSM and field measured

A t-test was conducted to compare AGB obtained from QSM tree volume and estimated by the allometric equation using tree parameters. There was no significant difference between AGB estimated from field measured tree parameters by an allometric equation using specific wood density (M=116.86) and AGB estimated from tree volume derived from QSM (M=122.92). Similarly, there is no significant difference between AGB estimated using generic wood density (mean=94.59 & 90.76) from field measured, and QSM derived tree volume respectively. Based on the result obtained from both methods the null hypothesis is accepted at 95 % confidence interval ($\alpha = 0.05$).

3.3.8. The Relationship between AGB derived from QSM and TLSpoint clouds

Diameter at breast height and height of individual trees were extracted and measured using measuring tools in RiSCAN PRO to estimate AGB/carbon stock using generic wood density allometric equation and specific wood density allometric equation from global wood density. The allometric equation used was from Chave et al. (2005). Estimation of AGB/carbon stock obtained from QSM done by multiplying total tree volume generated through reconstruction algorithm with specific wood density 0.6987 and 0.8814 for *Avicennia* and *Rhizophora* respectively and 0.57 for generic wood density for both species. AGB derived from TLS with allometric equation was compared with AGB derived from QSM. Figure 27 and 28 show the relationship between AGB derived from TLS and derived from QSM with a coefficient of determination (R^2) 0.976 and 0.974 for general and specific wood density respectively. These results suggest that wood density does not significantly affect the estimation of AGB using QSM derived tree volume and TLS derived tree parameters (Appendix 8).

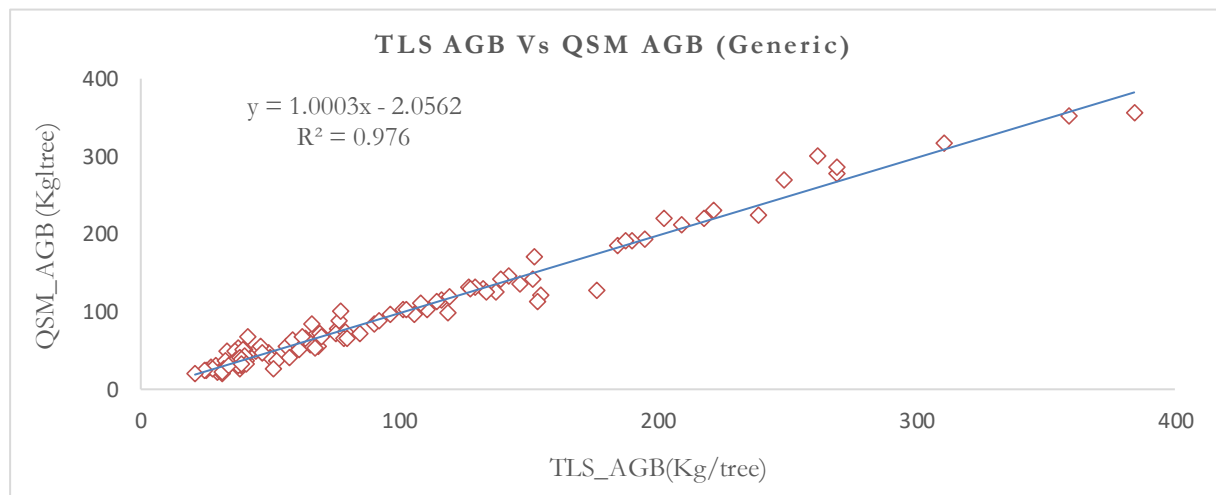


Figure 28. The relationship between AGB derived from QSM and derived from TLS using general wood density.

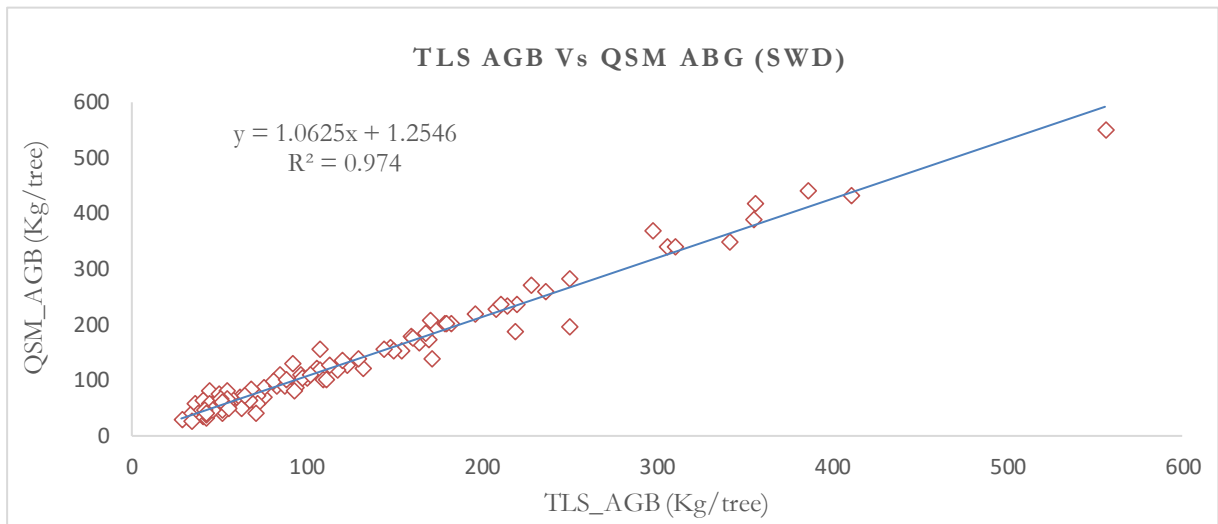


Figure 29. The relationship between TLS and QSM derived AGB using specific wood density.

4. DISCUSSION

4.1. Application of Quantitative Structure Model (QSM) to Estimate AGB in Mangrove Forest.

Mangroves forests are the most carbon-rich forest and have a triplicate potential in carbon sequestration as compared to the tropical inland forest (Donato et al., 2011). Accurate measurement of AGB of forest is essential to show its role in global climate change. Assessment of forest AGB/carbon stock by TLS using QSM is one way to support climate change mitigation strategy. This method applied in the temperate and tropical forests to assess AGB/carbon stock, but there is no research work done yet on the assessment of mangrove forest AGB/carbon stock by TLS using QSM. However, comparatively mangrove forests are carbon-rich than inland forest and have potential in climate change mitigation. Therefore, applying this method (i.e., QSM) to accurately assess the AGB/carbon stock of mangrove forest and implemented and investigated as a new technique has encouraged me to do this research work. Consequently, the result of this research work can be presented to REDD+ RMV as one of the techniques that can be recommended to the countries who will assess their AGB/carbon stock for evaluating climate change. Furthermore, it can be used to assess AGB/carbon stock and prove that a country has more carbon stock than emission and applying for the payment compensation from the UN.

The result of this study shows that TLS point clouds have a great potential to estimate the volume of mangrove forest which can be used for biomass estimation. The AGB/carbon stock of mangrove forest using QSM were estimated via tree volume multiplied by its wood density. The results indicated that there is no significant difference between AGB/carbon stock derived from QSM and field-measured tree parameters (i.e., DBH and height). This result suggests that QSM is as accurate as the standard reference method used to assess AGB/carbon stock using the allometric equation. However, mangrove forest trees in the study area of this research are young, the tree height is not too high, and its canopy structure is relatively open. Therefore, I propose to apply this method in a dense mangrove forest and combine with airborne lidar data to see the difference when using the allometric equation. The critical details of the methods and activities used in this study are discussed in the following sections.

4.2. DBH measurement and sources of error.

Trees DBH is a critical measurement of forest inventory, and it is a vital predictor for biomass and carbon stock (Yao et al., 2011). Laar & Akça, (2007) stated that measuring DBH using diameter tape produced biased estimates if the stem is not perfectly circular. Errors are observed mainly in large trees where it is difficult to verify the position of the diameter tape at the back of the trees. The problem that we faced when we measured DBH in this study using diameter tape was tree climbing that has prop roots (i.e., *Rhizophora* species) (Figure 30). DBH measured as the horizontal distance at 1.3 m above the ground for *Aveceian* species and 0.2 to 0.3 m above the highest prop roots in case of *Rhizophora* species. DBH extracted from point cloud was validated using DBH measured from the field. The DBH derived from TLS was highly correlated with DBH measured from the field R^2 of 0.978 with RMSE of 0.62 cm, which is consistent with previous work done by Madhibha, (2016) and Maassa, (2018) in the tropical forest using TLS.



Figure 30. Mangrove forest with prop roots that challenges measuring the diameter at breast height, movement within the plot and TLS installation in addition to ecological challenges (e.g., tide, mud, etc.).

Madhibha, (2016) and Maassa, (2018) used TLS to assess above ground biomass in the tropical rainforest using QSM and came up with R^2 0.993 with RMSE of 1.1cm and R^2 0.989 with RMSE of 1.37cm respectively. In both cases, the R^2 is slightly higher than in this study because both types of research performed their work on inland forest whereas this research carried out on coastal mangrove forest. From an ecological standpoint as well as biophysical characteristics and landscape, mangrove is entirely different from the tropical in-land forest. Mangrove ecology is different than tropical forest since it grows in flat coastal landscape (Luttge, 2008). The muddy soil and water cover it almost continuously with high and low tide throughout the day and night time, and the prop root of *Rhizophora* species makes the DBH measurement tough and TLS installation inside the sample plot (Figure 9). Moreover, to reduce the risk of occlusion intensive undergrowth clearing was done before start scanning in all scanning positions.

Some researches done in tropical forest show a similar result. Zulkarnain et al. (2017) got R^2 of 0.969 with RMSE of 0.062 cm during their study of estimating AGB of an individual tree; they used four scanning positions of TLS. These imply that when multiple scanning positions are applied, it is easy to assess the structure of the tree, and DBH measurement is accurate. Underestimation of individual tree DBH occurred as a result of two reasons. First by cylinder fitting in which cylinders were fitted to the inner side of the point clouds and the second one is due to uneven distribution or occlusion of point cloud that causes the primary problem for the improper fitting of the cylinder which results in a small error in DBH estimation (Figure 31) (Zulkarnain et al., 2017).

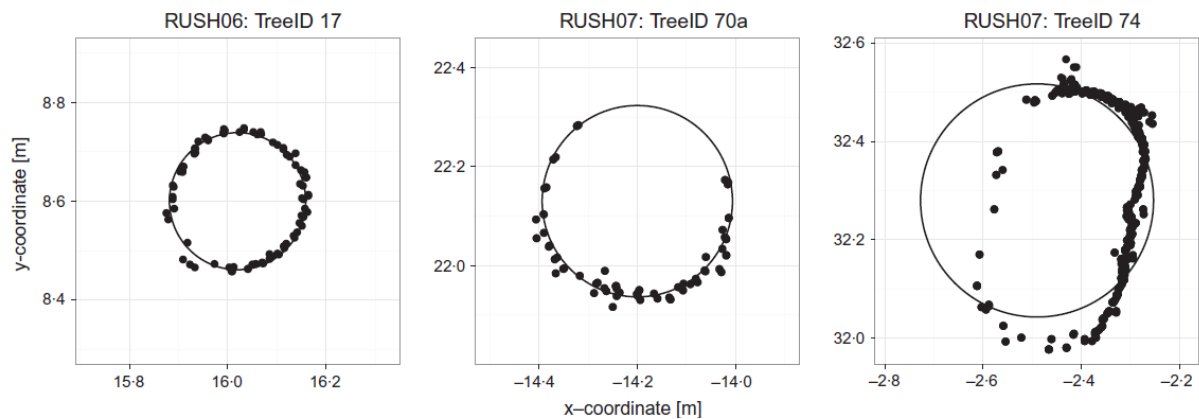


Figure 31. TLS derived DBH through circular fitting method. No occlusion (left), Partial occlusion (middle) and not an optimal fit circle (right) (Calders et al., 2015)

4.2.1. Distribution of field measured DBH, and TLS derived DBH

Measurement and recording of DBH for all trees in 30 plots during the fieldwork were done. The distribution data of tree measurements of DBH from TLS and DBH from field analysed. DBH derived from TLS and field measured DBH were examined and showed that they are not normally distributed, i.e., positively skewed. As Knox et al. (1989) stated positive skewness of the data shows the tail is longer to the right side than the left side, which is similar to the result of this study (Appendix 8). The main reason for the skewness of the DBH measurements positively is because we only consider trees that have a DBH ≥ 10 cm. Trees that had DBH < 10 cm not included. Its contribution to the biomass of a tree within the plot is insignificant (Brown, 2002). This result is the same with Maassa, (2018) when he looks at the distribution of DBH measured from the field and DBH derived from TLS.

4.3. Tree height measurement accuracy and source of error

In this study, the height measurement of mangrove trees using TLS and handheld laser instrument (Leica DISTO D510 laser ranger) are not significantly different (Figure 23). This finding contrasts with the result from Ayer Hitam Tropical Forest of Malaysia (Madhibha, 2016). The linear regression between the field measured height and TLS derived height in this study shows R^2 of 0.73 with RMSE of 1.93 m. Whereas, the result of Madhibha, (2016) which comparatively lower than this research was R^2 of 0.59 with RMSE 3.4 m due to the nature of the study area. The mangrove forest in this study area are young, and the density of canopy is much lower than the tropical forest (Figure 31). In the case of Madhibha, (2016) it is a dense forest with intermingling canopy.

Dassot et al. (2011) observed that inaccuracies in height measurement in high canopy conditions which are challenging to identify the top of the tree because of getting the laser beam of Leica to hit the very top of the tree. But it is not true in our case due to the open canopy structure of mangrove forest in the study area. However, tree movement by wind and appropriate distance from the tree leads to an approximation of the

tree top. Consequently, it resulted in an overestimation of the tree height by 0.35 m. As Bazezew, (2017) indicated the accuracy of height measurement by Leica related to the distance from the tree. He stated that 20 to 30 m distance is reasonable to see the top of the tree. In reality, it was difficult in the mangrove ecosystem because of the occlusion and the movement inside the plot (blockage of prop root, the problem of a stand and walk in the mud and water).

The height of tree derived from TLS was measured in RiSCAN PRO software using measuring tools, which is the distance between highest and lowest terrestrial LiDAR point cloud of individual tree and compared with field measured height using Leica. TLS and RiSCAN techniques are very accurate (Bazezew, 2017). The openness of mangrove forest canopy in the study area helps to scan the top of the tree by TLS and Leica laser beam to hit the tree top. Thus why the relationship between both TLS and Leica based height measurement was significant as compared to the inland tropical forest where the tree canopies are intermingling and challenging to scan the top of the tree either by TLS or Leica due to occlusion.



Figure 32. Young and open canopies of mangrove forest which is assessable to the laser beam to reach the top of the tree to measure tree height in the study area.

4.4. Acquisition and Registration of point clouds

During data collection, we used multiple scanning positions. The setup of TLS was at an angle of 120 degrees relative to each other in the outer scanning positions. In reality, it was difficult and not always achieved due to mud, water, prop root of *Rhizophora* and unstable nature of the ground in the area. The point clouds in all scanning positions were merged into a single data set with the help of retroreflectors that placed in a location where it was visible to at least two scanning positions. Circular (6) and cylindrical (12) total 18 reflecting targets used in this study which were distributed uniformly throughout the sample plot (Figure 7). Time of scanning and numbers of reflectors has a direct relationship. When the number of reflecting targets is higher, it takes more time to scan. According to Maas et al. (2008) as the number of targets increased the accuracy of registration scan also increased. To have high accuracy Bienert et al. (2006) used a total of 19 retroreflectors for registration, finally, they achieved.

The beam divergence that related to the density of point cloud acquired is one source of error (Okatani & Deguchi, 2002). In this study, a panorama 40 scanning mode used which gives dense point cloud, but it takes more time when compared with panorama 60. The time it took when panorama 40 applied was 8 to 10 minutes whereas for panorama 60 it took 3 to 4 minutes. Therefore, the number of retroreflector, scanning mode and multiple scanning positions around the individual trees are needed to be high enough and adequate to catch the detail of trees structure.

4.5. Individual tree extraction

About 350 of trees were identified and extracted from registered point cloud data. Manual extraction of the tree is tedious to remove noise and points which are not a part of the tree structure. However, the method we used to extract a tree has also its influence on the cleaning of point cloud which is not part of the tree (Figure 33). Adewole et al. (2016) in a similar way they stated that extraction of an individual tree is a time consuming, and they confirmed that depending on the structure of the mangrove forest it takes 1 to 12 hrs. Figure 33 shows a top view (641,599 points) extraction and bottom view (434,528 points) extraction of the same tree with a difference of 207,071 point clouds that need to clean. On top of that, when we apply top view extraction, it is challenging to include all the branches. As indicated in figure 33 narrow at the top and broader at the bottom that excludes some branches and vice versa when applying bottom view extraction.

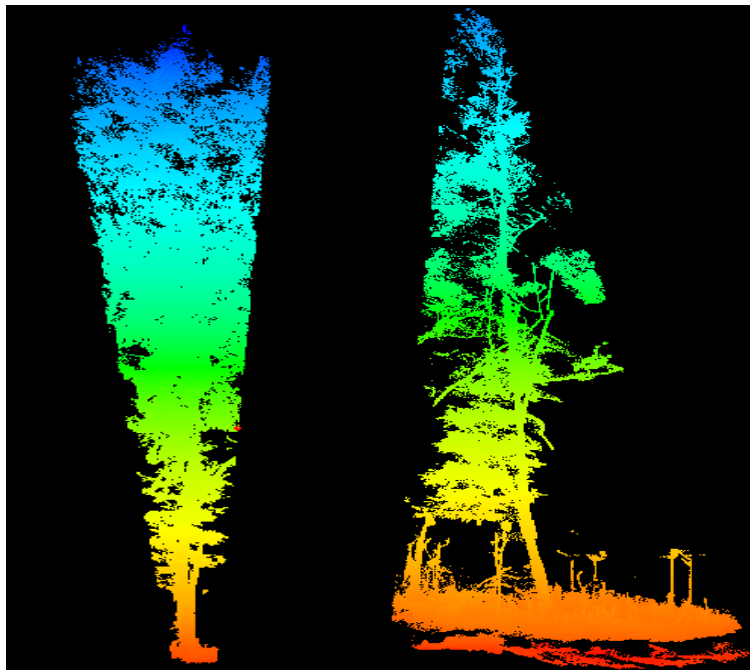


Figure 33. Bottom view (left) and top view (right) manually extracted individual trees from TLS point clouds.

4.6. Wood density

In this study to estimate AGB, both specific and general wood density were used as an input in the allometric equations to see its influence on the AGB estimated. There is no significant difference between AGB estimated by either of FAO default or specific wood density. Calders et al. (2015) used average wood density that sampled across a range of DBH measurements to estimate AGB, and they stated that the use of average wood density which resulted from a range of DBH introduce uncertainty in the conversion of volume to aboveground biomass. However, in this study, one wood density was applied to the whole trees and showed no significant difference.

4.7. Above Ground Biomass/Carbon Stock Accuracy Assessment test

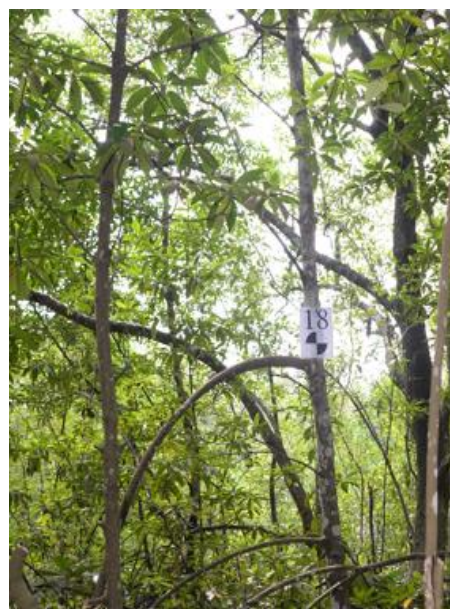
4.7.1. Field measured AGB compared with AGB derived from TLS

Assessing the accuracy of AGB derived from TLS concerning field measured is part of this research. AGB estimated using field-measured tree parameters are considered as accurate and used to assess the accuracy of AGB derived from TLS. This research showed that there is no significant difference between AGB estimated from field measured DBH and height with AGB estimated using TLS derived DBH and height. In both method measurement of DBH and tree height were not difficult in the study area due to the young and open canopy of the mangrove forest. The mean variation of AGB derived from TLS and AGB estimated from the field is 1.8 kg/tree and 2.36 kg/tree using general and specific wood density respectively. Ghebremichael, (2015); Bazezew, (2017) and Maassa, (2018) also compared AGB derived from TLS with field measured and he has got the same result in tropical inland forests.

4.7.2. Field measured AGB compared with AGB derived from QSM

One of the research questions of this study was to find out the accuracy of AGB derived from QSM as compared to field measured AGB. There is no significant difference between AGB derived from QSM compared to AGB from field-measured. The young mangrove forest, no intermingling or overlap nature of the canopy and less undergrowth vegetation cover have shown a significant contribution for the obtained result. As this method is new to mangrove forest, I did not find previous work done on mangrove forest that assesses AGB by TLS using QSM. Thus, I compared the result of this study with an inland tropical forest that applies the same method.

Madhibha, (2016) used field-measured tree parameters and TLS point cloud to estimate AGB of tropical forest in Ayer Hitam Forests Reserve, Malaysia and she got coefficient of determination or R^2 of 0.81 using default wood density and R^2 of 0.797 for species-specific wood density which is slightly different with the R^2 of 0.9638 for generic and R^2 of 0.9649 for specific wood density in this study. The difference happened due to more young trees and open canopies of mangrove. In the same time the trees in the mangrove were not very high and intermingling in this study area. Thus, it was easier for the laser beams of the TLS to reach the stems and canopies of the trees, and consequently, the point clouds were able to estimate the tree parameters better than the tropical in-land forest. Therefore, the AGB in this study estimated with higher accuracy as compared to the tropical inland forest.



Ayer Hitam Tropical Forest (Madhibha, 2016) Tani Baru young tropical mangrove forest (current study)
Figure 34. Closed canopy tropical forest (left) and young open mangrove forest (right).

4.7.3. Above ground biomass derived from QSM compared with AGB derived from TLS

Comparing the difference between AGB derived from QSM with AGB derived from TLS was the initiation of this research. Accordingly, the findings of the study which showed that there is no significant difference between AGB derived from QSM compared with AGB derived from TLS. As the reconstruction of the tree in QSM depends on the point cloud from the TLS, these results were expected. Tilon, (2017) and Maassa, (2018) found the same result with this research when they compare AGB derived from QSM and TLS in the tropical and temperate forest because QSM depends on TLS point cloud. However, Madhibha, (2016) get a significant difference when she compared AGB derived from tree QSM that had canopy biomass greater than trunk biomass with AGB derived from TLS. The major contributor to error which affects AGB derived from QSM tree volume is when the canopy volume is greater than the trunk volume. Which may happen due to the intermingling of the canopy, appropriate selection of QSM parameter and removal of non-woody materials during filtering. This problem does not exist in this study. Therefore, the relation between AGB derived from QSM and AGB derived TLS is accurately high.

5. CONCLUSION AND RECOMMENDATION

5.1. Conclusion

This study explored the applicability of TLS using Quantitative Structure Modelling (QSM) to estimate AGB/carbon stock in the mangrove forest of the Delta of Mahakam River, East Kalimantan, Indonesia. Estimating AGB/carbon stock of mangrove forest by TLS using QSM was successfully done and showed comparable results with field measured AGB and TLS derived AGB. Activities such as intensive cleaning, multiple scans and equal distribution of reflectors that reduce registration error contribute to high accuracy in assessing AGB/carbon stock in this study.

Even though the area is inaccessible, the fieldwork was tough and difficult to carry TLS in mud, high tide and struggling with a dangerous animal such as Crocodiles which makes the activities extremely difficult and in the same time applying QSM model in mangrove forest is very innovative. The analysis of this study shows point clouds which generated from TLS can effectively be used in QSM to estimate AGB/carbon stock of mangrove forest in the coastal area. Consequently, based on the results, the research question stated at the beginning of this thesis are answered as followed:

1. What is the relation between tree height and DBH derived from field measurement and derived from TLS?

DBH and tree height measured in the field were highly correlated with DBH and tree height derived from TLS. Thus, there is no significant difference between TLS derived, and field measure DBH and height measurements. Therefore, the null hypothesis accepted at a 95% confidence interval.

2. How accurate is AGB/carbon stock derived from TLS compared with AGB/carbon stock estimated from field measurements?

The finding of the study suggests that the estimation of AGB derived from TLS was highly correlated with AGB estimated from field measurements. Consequently, the null hypothesis is accepted at 95% confidence interval.

3. What is the relationship between AGB/carbon stock derived from TLS and AGB/carbon stock from QSM?

The finding in this showed that there is no significant difference between AGB derived from QSM compared with AGB derived from TLS. Therefore, the null hypothesis was accepted at 95% confidence interval.

4. How accurate is AGB/carbon stock derived from TLS using QSM compared with AGB/carbon stock estimated from field-measured tree parameters by the allometric equation?

The results showed that the relationship between AGB/carbon stock derived from QSM and field measurements using the allometric equation are highly correlated. The results of this study show that QSM can accurately estimate AGB/carbon stock of mangrove forest in the coastal area. Therefore, the null hypothesis was accepted at 95% confidence interval.

5.2. Recommendation

- ✓ Extraction of an individual tree from the bottom is vital to minimising point cloud which is not part of the tree, and other trees point cloud. Therefore, a bottom view is better for tree extraction.
- ✓ In the coastal area, especially in mangrove forest, it is difficult to install tripod on which TLS mount and due to the unstable nature of the area. Therefore, it is better to use another type of TLS that doesn't require a tripod, e.g., back-bag mobile laser scanning.
- ✓ Assessment of AGB/carbon stock of mangroves with TLS using QSM needs to be tested in other areas where the mangrove forests are old, and their canopies are intermingling combined with airborne LiDAR.

REFERENCES

- Abegg, M., Kükenbrink, D., Zell, J., Schaeppman, M. E., & Morsdorf, F. (2017). Terrestrial laser scanning for forest inventories-tree diameter distribution and scanner location impact on occlusion. *Forests*, 8(6), 1–29. <https://doi.org/10.3390/f8060184>
- Adewole, O., Proisy, C., Féret, J.-B., Blanchard, E., Fromard, F., Mehlig, U., ... Berger, U. (2016). Extended biomass allometric equations for large mangrove trees from terrestrial LiDAR data. *HAL Archives-Ouvertes.Fr*, 30(3), 935–947. <https://doi.org/10.1007/s00468-015-1334-9>
- Akerblom, M. (2012). Quantitative tree modelling from laser scanning data (M.Sc. Thesis). *Tampere University of Technology*, 88. Retrieved from <https://dspace.cc.tut.fi/dpub/handle/123456789/21012>
- Akerblom, M., Raunonen, P., Mikko, K., & Eric, C. (2015). Analysis of Geometric Primitives Quantitative Structure Models of Tree Stems. *Remote Sensing*, 7(4), 4581–4603. <https://doi.org/10.3390/rs70404581>
- Alongi, D. M. (2008). Mangrove forests: Resilience and protection from tsunamis, and responses to global climate change. *Estuarine, Coastal and Shelf Science*, 76(1), 1–13. <https://doi.org/10.1016/j.ecss.2007.08.024>
- Basuki, T. M., Laake, P. E., Skidmore, A. K., & Hussin, Y. A. (2009). Forest Allometric equations for estimating the above-ground biomass in tropical lowland Dipterocarp forests. *Forest Ecology and Management*, 257(8), 1684–1694. <https://doi.org/10.1016/j.foreco.2009.01.027>
- Bazew. N, M. (2017). Integrating Airborne LiDAR and Terrestrial Laser Scanner Forest Parameters for accurate estimation of above ground biomass/carbon stock in Ayer Hitam Tropical Forest Reserve, Malaysia (MSc. Thesis). *The University of Twente, Faculty of Geo-Information Science and Earth Observation, Natural Resource Management*. Retrieved from https://library.itc.utwente.nl/papers_2017/msc/nrm/bazew.pdf
- Béland, M., Baldocchi, D. D., Widlowski, J., Fournier, R. A., & Verstraete, M. M. (2014). On seeing the wood from the leaves and role of voxel size determining leaf area distribution of forests with terrestrial LiDAR. *Agricultural and Forest Meteorology*, 184, 82–97. <https://doi.org/10.1016/j.agrformet.2013.09.005>
- Bienert, A., Maas, H., & Scheller, S. (2006). Analysis of the Information Content of Terrestrial Laser Scanner Point Clouds for the Automatic Determination of Forest Inventory Parameters.
- Bosma, R., Sidik, A. S., van Zwieten, P., Aditya, A., & Visser, L. (2012). Challenges of a transition to sustainably managed shrimp culture agro-ecosystem in the Mahakam, East Kalimantan, Indonesia. *Wetlands Ecology and Management*, 20(2), 89–99. <https://doi.org/10.1007/s11273-011-9244-0>
- Bouillon, S. et al. (2008). Mangrove forest production and carbon sinks: A revision of global budget estimates. *Global Biogeochemical Cycles*, 22(2). <https://doi.org/10.1029/2007GB003052>
- Brown, S. (2002). Measuring Carbon Forests: Current status and future challenges. *Environmental Pollution*, 116(3), 363–372. [https://doi.org/10.1016/S0269-7491\(01\)00212-3](https://doi.org/10.1016/S0269-7491(01)00212-3)
- Calders, K. et al. (2015). Non-destructive estimates of above-ground biomass using terrestrial laser scanning, 198–208. <https://doi.org/10.1111/2041-210X.12301>
- Chave, J. et al. (2005). Tree allometric equation and improved estimation of carbon stocks and balance in tropical forests. *Oecologia*, 145(1), 87–99. <https://doi.org/10.1007/s00442-005-0100-x>
- Chave, J. et al. (2014). Improved allometric models to estimate aboveground biomass of tropical trees. *Global Change Biology*, 20(10), 3177–3190. <https://doi.org/10.1111/gcb.12629>
- Comley, B. & McGuinness, K. (2005). Above and below-ground biomass, and allometry, of four common northern Australian mangroves. *Australian Journal of Botany*, 53(5), 431–436. <https://doi.org/10.1071/BT04162>
- Coronado Molina, C., Day, J. W., Reyes, E., & Perez, B. C. (2004). Standing crop and above ground biomass partitioning of a dwarf mangrove forest in Taylor River Slough, Florida. *Wetlands Ecology and Management*, 12(3), 157–164. <https://doi.org/10.1023/B:WETL.0000034071.17156.c0>
- Dassot, M., Constant, T., & Fournier, M. (2011). Use of terrestrial LiDAR technology in forest science: Application on fields, benefits and challenges. *Annals of Forest Science*, 68(5), 959–974. <https://doi.org/10.1007/s13595-011-0102-2>
- Dittmar, T., Kattner, G., Hertkorn, N., & Lara, R. J. (2006). The mangrove forest, a major source of dissolved organic carbon to the oceans. *Global Biogeochemical Cycles*, 20(1), 1–7. <https://doi.org/10.1029/2005GB002570>

- Donato, D. C. et al., (2011). Mangrove forests are among the most carbon-rich forests in the tropics. *Nature Geoscience*, 4(5), 293–297. <https://doi.org/10.1038/ngeo1123>
- Drake, J. B. et al., (2003). Above ground biomass estimation in closed canopy of Neotropical forests using LiDAR remote sensing: factors. *Global Ecology and Biogeography*, 147–159. <https://doi.org/10.1046/j.1466-822X.2003.00010.x>
- Duarte, C. M., Losada, I. J., Hendriks, I. E., Mazarrasa, I., & Marbà, N. (2013). The role of coastal plant communities for climate change mitigation and adaptation. *Nature Climate Change*, 3(11), 961–968. <https://doi.org/10.1038/nclimate1970>
- Duke, N. C., Meynecke J.O, Dittmann S, Ellison A.M, Anger K, et al. (2007). A World Without Mangroves? *Science*, 317(July), 41–43. <https://doi.org/10.1126/science.317.5834.41b>
- FFPRI. (2012). How to measure and monitor forest carbon. Retrieved from http://theredddesk.org/sites/default/files/resources/pdf/redd_cookbook_all_low_en_1.pdf.
- FAO. (2007). The world's mangroves 1980-2005. *FAO Forestry Paper*, 153, 89. <https://doi.org/978-92-5-105856-5>
- FAO. (2017). What is REDD+?
- Feliciano. E., et al., (2014). Assessment of mangrove aboveground biomass and structure using Terrestrial Laser Scanning: A case study in the Everglades National Park. *Wetlands*, 34(5), 955–968. <https://doi.org/10.1007/s13157-014-0558-6>
- Ghebremichael, Z. M. (2015). Airborne LiDAR and Terrestrial Laser Scanner (TLS) in Assessing Above Ground Biomass/Carbon Stock in Tropical Rainforest of Ayer Hitam Forest Reserve, Malaysia (MSc. Thesis). *The University of Twente, Faculty of Geo-Information Science and Earth Observation, Natural Resource Management.*, 67. Retrieved from http://www.itc.nl/library/papers_2016/msc/nrm/ghebremichael.pdf
- Gibbs, H. K., et al., (2007). Monitoring and estimating the tropical forest carbon stocks: Making REDD+ a reality. *Environmental Research Letters*, 2(4). <https://doi.org/10.1088/1748-9326/2/4/045023>
- Giri, C. et al., (2011). The status and distribution of mangrove forests of the world using earth observation satellite data. *Global Ecology and Biogeography*, 20(1), 154–159. <https://doi.org/10.1111/j.1466-8238.2010.00584.x>
- Hackenberg, J. et al., (2014). The highly accurate tree models derived from TLS data: A method description. *Forests*, 5(5), 1069–1105. <https://doi.org/10.3390/f5051069>
- Hackenberg, J. et al., (2015). A non-destructive method for biomass prediction combining TLS derived tree volume and wood density. *Forests*, 6(4), 1274–1300. <https://doi.org/10.3390/f6041274>
- Hess, C., Bienert, A., & Hä, W. (2015). Wood Volume Estimates of Single Young Trees by Terrestrial, m, 3847–3867. <https://doi.org/10.3390/f6113847>
- Hill, T. C., Williams, M., Bloom, A. A., Mitchard, E. T. A., & Ryan, C. M. (2013). Are Inventory Based and Remotely Sensed Above-Ground Biomass Estimates Consistent? *PLoS ONE*, 8(9), 1–8. <https://doi.org/10.1371/journal.pone.0074170>
- Houghton, R. A., Hall, F., & Goetz, S. J. (2009). Importance of biomass in the global carbon cycle. *Journal of Geophysical Research: Biogeosciences*, 114(3), 1–13. <https://doi.org/10.1029/2009JG000935>
- IPCC. (2006). The 2006 IPCC guidelines for national greenhouse gas inventories. *Institute for Global Environmental Strategies (IGES), Hayama, Japan on Behalf of the IPCC*, 4.
- Kangkuso, A., Sharma, S., Jamily, J., Septiana, A., Sahidin, I., Rianse, U., ... Nadaoka, K. (2018). Trends in allometric models and aboveground biomass of family *Rhizophoraceae* mangroves in the Coral Triangle ecoregion, Southeast Sulawesi, Indonesia. *Journal of Sustainable Forestry*, 37(7), 691–711. <https://doi.org/10.1080/10549811.2018.1453843>
- Knox, R. G., Peet, R. K., & Christensen, N. L. (1989). Population dynamics in loblolly pine stands changes in skewness and size inequality. *Ecology*, 70(4), 1153–1166. <https://doi.org/10.2307/1941383>
- Köhl, M., Magnussen, S. S., & Marchetti, M. (2006). *Sampling Methods, Remote Sensing and GIS Multiresource Forest Inventory*. Springer Science & Business Media ISBN 3540325727. Retrieved from <https://books.google.com/books?hl=en&lr=&id=uspzLjVWNgMC&pgis=1>.
- Komiyama, A., Pongpam, S., & Kato, S. (2005). Common allometric equations to estimating the tree weight of mangroves. *Journal of Tropical Ecology*, 21(4), 471–477. <https://doi.org/10.1017/S0266467405002476>
- Kristensen, E., Bouillon, S., Dittmar, T., & Marchand, C. (2008). Organic carbon dynamics in mangrove forest ecosystems: A review. *Aquatic Botany*, 89(2), 201–219. <https://doi.org/10.1016/j.aquabot.2007.12.005>

- Krooks, A., Kaasalainen, S., Kankare, V., Joensuu, M., Raunonen, P., & Kaasalainen, M. (2014). Tree structure vs height from terrestrial laser scanning and quantitative structure models. *Silva Fennica*, 48(2), 1–11. <https://doi.org/10.14214/sf.1125>
- Laar, A. van, & Akça, A. (2007). *Forest Mensuration* (Vol. 13). Dordrecht: Springer Netherlands. <https://doi.org/10.1007/978-1-4020-5991-9>
- lackmann.s. (2011). Expert meeting on assessment of forest inventory approaches for REDD +, (June), 1–18.
- Liang, X. et al. (2016). Automatic forest inventory parameter determination from TLS Data. *International Journal of Remote Sensing*, 29 (5), pp.1579-1593. Available at: <https://www.tandfonline.com/doi/abs/10.1080/01431160701736406>.
- Lu, D. (2006). The potential and challenge of remote sensing based aboveground biomass estimation. *International Journal of Remote Sensing*, 27(7), 1297–1328. <https://doi.org/10.1080/01431160500486732>
- Luttge, U. (2008). *Physiological Ecology of Tropical Plants (second)*. Darmstadt, Germany: Springer Berlin Heidelberg. | 9783662033401 | Boeken. Retrieved from <https://www.bol.com/nl/p/physiological-ecology-of-tropical-plants>
- Maas, H. G. et al. (2008). Automatic forest inventory parameter determination from TLS. *International Journal of Remote Sensing*, 29(5), 1579–1593. <https://doi.org/10.1080/01431160701736406>
- Maassa, E. J. (2018). The effect of tree density on the assessment of above ground biomass using Terrestrial Laser Scanner and Quantitative Structure Modelling in Berkelah Tropical Forest, Malaysia (MSc. Thesis). *The University of Twente, Faculty of Geo-Information Science and Earth Observation, Natural Resource Management*.
- Madhibha Tasiyiwa, P. (2016). Assessment of Above Ground Biomass with Terrestrial LiDAR using 3D Quantitative Structure Modelling in Tropical Rainforest of Ayer Hitam Forest Reserve, Malaysia (MSc. Thesis). *The University of Twente, Faculty of Geo-Information Science and Earth Observation, Natural Resource Management*.
- Mitchard, E. T. A., Feldpausch, T. R., Brienen, R. J. W., Lopez-Gonzalez, G., Monteagudo, A., Baker, T. R., ... Phillips, O. L. (2014). Markedly divergent estimates of Amazon forest carbon density from ground plots and satellites. *Global Ecology and Biogeography*, 23(8), 935–946. <https://doi.org/10.1111/geb.12168>
- Næsset, E. et al., (2004). Laser scanning of the forest: The Nordic experience. *Scandinavian Journal of Forest Research*, 19(6), 482–499. <https://doi.org/10.1080/02827580410019553>
- Nagelkerk, I et al., (2008). The habitat function of mangroves forest for terrestrial and marine fauna: A review. *Aquatic Botany*, 89(2), 155–185. <https://doi.org/10.1016/j.aquabot.2007.12.007>
- Newnham, G. J. et al. (2016). Erratum to: Terrestrial Laser Scanning for Plot-Scale Forest Measurement. *Current Forestry Reports*, 2(3), 214–214. <https://doi.org/10.1007/s40725-016-0039-7>
- Okatani, I. S., & Deguchi, K. (2002). A Method for Fine Registration of Multiple View Range Images Considering the Measurement Error Properties. *Cvii*, 87(1-3), 66–77. doi:10.1006/cvii.2002.0983.
- Olschofsky, K., Mues, V., & Köhl, M. (2016). An operational assessment of aboveground tree volume and biomass by terrestrial laser scanning. *Computers and Electronics in Agriculture*, 127, 699–707. <https://doi.org/10.1016/j.compag.2016.07.030>
- Ong, J. E., Gong, W. K., & Wong, C. H. (2004). The Allometry and Partitioning of the Mangrove, *Rhizophora apiculata*. *Forest Ecology and Management*, 188(1–3), 395–408. <https://doi.org/10.1016/j.foreco.2003.08.002>
- Othmani, A., Lew, L. F. C., Voon, Y., Stolz, C., & Piboule, A. (2013). Single tree species classification from Terrestrial Laser Scanning data for forest inventory. *Pattern Recognition Letters*, 34(16), 2144–2150. <https://doi.org/10.1016/j.patrec.2013.08.004>
- Palacz, A. P., St. John, M. A., Brewin, R. J. W., Hirata, T., & Gregg, W. W. (2013). Distribution of phytoplankton functional types in high-nitrate, low-chlorophyll waters in a new diagnostic ecological indicator model. *Biogeosciences*, 10(11), 7553–7574. <https://doi.org/10.5194/bg-10-7553-2013>
- Persoon, G. A., & Simarmata, R. (2014). Undoing “marginality”: The islands of the Mahakam Delta, East Kalimantan (Indonesia). *Journal of Marine and Island Cultures*, 3(2), 43–53. <https://doi.org/10.1016/j.imic.2014.11.002>
- Pfeifer, N., Gorte, B., Winterhalder, D., Sensing, R, & Range, C. (2004). Automatic Reconstruction of Single TLS Scanner Data. In *20th ISPRS Congress 114-119* (Vol. 35, pp. 1–6). It retrieved from http://www.isprs.org/congresses/beijing2008/proceedings/5_pdf/81.pdf.

- Pham, T. D., Yokoya, N., Bui, D. T., & Yoshino, K. (2019). Remote Sensing Approaches for Monitoring Mangrove Species, Structure, and Biomass: Opportunities and Challenges, 1–24. <https://doi.org/10.3390/rs11020230>
- Popescu, S. C., Zhao, K., Neuenschwander, A., & Lin, C. (2011). Satellite LiDAR vs small footprint airborne LiDAR: Comparing the accuracy of above ground biomass estimates and forest structure metrics at footprint level. *Remote Sensing of Environment*, 115(11), 2786–2797. <https://doi.org/10.1016/j.rse.2011.01.026>
- Pretzsch, H. (2009). *Forest Dynamics, Growth and Yield. Mosaic A Journal For The Interdisciplinary Study Of Literature*. <https://doi.org/10.1007/978-3-540-88307-4>
- Raunonen, P. et al., (2013). A fast automatic method for constructing topologically and geometrically precise tree models from TLS Data. *International Conference on Function-Structural Plant Models (June)*, 89–91. doi:10.13140/2.1.4259.9206
- Raunonen, P. (2015). Quantitative structure tree models from terrestrial laser scanner data, (September), 28–30.
- Raunonen, P. (2017). TreeQSM Quantitative Structure Models of Single, (August).
- RIEGL. (2014). RIEGL VZ-400, 3–6.
- Ruiz-Peinado Gertrudix, R., Montero, G., & Del Rio, M. (2012). Biomass models to estimate carbon stocks for hardwood tree species. *Forest Systems*, 21(1), 42. <https://doi.org/10.5424/fs/2112211-02193>
- Ruiz, L. A., Hermosilla, T., Mauro, F., & Godino, M. (2014). Analysing the influence of plot size and LiDAR density on forest structure attribute estimates, *Forests*, 5(5), 936–951. doi:10.3390/f5050936.
- Schwieder, M. et al., (2018). Landsat phenological metrics and their relation to above ground carbon in the Brazilian Savanna. *Carbon Balance and Management*, 13(1), 1–15. <https://doi.org/10.1186/s13021-018-0097-1>
- Smith, T. J., & Whelan, K. R. T. (2006). Development of allometric relations for three mangrove forest species in South Florida for use in the Greater Everglades Ecosystem Restoration. *Wetlands Ecology and Management*, 14(5), 409–419. <https://doi.org/10.1007/s11273-005-6243-z>
- Sy, V., Herold, M., Beuchle, R., Clevers, J. G. P. W., Lindquist, E., & Vershot, L. (2015). Land use patterns and related carbon losses following deforestation in South America. *Environmental Research Letters*, 10, 1–14.
- Teddle, C., & Yu, F. (2007). Mixed Methods Sampling. *Journal of Mixed Methods Research*, 1(1), 77–100. <https://doi.org/10.1177/2345678906292430>
- The REDD Desk. (2017). Tanzania | The REDD Desk.
- Thies, M., & Spiecker, H. (2004). The evaluation and future prospects of Terrestrial Laser Scanning to Standardised Forest Inventories. *I*, 36(8/w2), 192–197. Retrieved from <http://www.isprs.org/proceedings/XXXVI/8-W2/THIES.pdf>
- Tilon, S. M. (2017). The effect of foliage on estimating above ground forest biomass using Terrestrial Laser Scanning and Quantitative Structure Modelling in Gronau, Germany (M.Sc. Thesis). *The University of Twente, Faculty of Geo-Information Science and Earth Observation, Natural Resource Management*, 73.
- Tomlinson, P. B. (Philip B. (1994). *The botany of mangroves*. Cambridge University Press. Retrieved from https://books.google.nl/books/about/The_Botany_of_Mangroves.html?id=uwT6SMY-oNAC&redir_esc=y
- Valiela, I., Bowen, J., & York, J.(2001). Mangroves are one of the world's threatened major tropical environments. *BioScience*, 51(10), 807. [https://doi.org/10.1641/0006-3568\(2001\)051\[0807:MFOOTW\]2.0.CO;2](https://doi.org/10.1641/0006-3568(2001)051[0807:MFOOTW]2.0.CO;2)
- Vashum, T., & Jayakumar, S. (2012). Methods to Estimate Above-Ground Biomass and Carbon Stock in Natural Forests - A Review. *Journal of Ecosystem & Ecography*, 02(04). <https://doi.org/10.4172/2157-7625.1000116>
- Vastaranta, M., Melkas, T., Holopainen, M., H., K., Hyypä, J., & Hyypä, H. (2009). Laser-Based Field Measurements in Tree-Level Forest Data Acquisition. *Photogrammetric Journal of Finland*, 21(2), 51–61.
- Wilkes, P. et al., (2017). Data acquisition for considerations of Terrestrial Laser Scanning forest plots. *Remote Sensing of Environment*, 196, 140–153. <https://doi.org/10.1016/j.rse.2017.04.030>
- Yao, T. et al., (2011). Remote Sensing of Environment Measuring forest structure and biomass in New England forest stands using Echidna ground-based lidar. *Remote Sensing of Environment*, 115(11), 2965–2974. <https://doi.org/10.1016/j.rse.2010.03.019>

- Yu, X. et al., (2013). A stem biomass estimation based on stem reconstruction from TLS point clouds. *Remote Sensing Letters*, 4(4), 344–353. <https://doi.org/10.1080/2150704X.2012.734931>
- Zianis, D. (2008). Predicting mean aboveground forest biomass and its associated variance. *Forest Ecology and Management*, 256(6), 1400–1407. <https://doi.org/10.1016/j.foreco.2008.07.002>
- Zianis, D., & Seura, S. (2005). A biomass and stem volume equations for tree species in Europe. *Silva Fennica Monographs* (Vol. 4). <https://doi.org/citeulike-article-id:11858948>
- Zulkarnain, M., Rahman, A., Bakar, A. A., Razak, K. A., Faidi, A., Kassim, A. R., & Latif, Z. A. (2017). Non-destructive, laser-based individual tree aboveground biomass assessment in a tropical forest. <https://doi.org/10.3390/f8030086>

LIST OF APPENDICES

Appendix 1: Field measurement sheet.

The data sheet for Borneo Island Mahakam River, East Kalimantan							
Author	Plot Radius	Slope %	date				
Plot center	Latitude:	Longitude:	Plot No:				
Canopy Density (%)							
Photography		Name of recorder					
Tree No:	Latitude	Longitude	Species	DBH (cm)	Height (m)	Crown diam.(m)	Canopy density (%)
1							
2							
3							
4							
5							
6							
7							
8							
9							
10							
11							
12							
13							
14							
15							
16							
17							
18							
19							
20							
21							
22							
23							
24							
25							
26							
27							
28							
29							
30							
31							

Appendix 2: QSM output.

tree_19.txt

All points: 254066, First filtering: 2004, Points left: 252062

All points: 252062, Second filtering: 33721, Points left: 218341

All points: 254066, All filtered points: 35725, Points left: 218341

.....

Tree attributes:

Total Volume = 174.3 L

Trunk Volume = 87.19 L

Branch Volume = 87.07 L

Tree Height = 13.12 m

Trunk Length = 12.51 m

Branch Length = 173.3 m

Number Branches = 351

Max Branch Order = 5

Total Area = 14.77 m²

DBHqsm = 0.1393 m

DBHcyl = 0.1305 m

DBHtri = 0.1393 m

Tria Trunk Volume = 87.19 L

Mix Trunk Volume = 87.19 L

Mix Total Volume = 174.3 L

Tria Trunk Length = 0 m

Average cylinder-point distance: 17.6 19.8 17.2 21.3 mm

Appendix 3: Descriptive statistics of the field and TLS DBH left to right

<i>Field DBH</i>	
Mean	15.19
Standard Error	0.30
Median	13.5
Mode	10
Standard Deviation	5.57
Sample Variance	31.00
Kurtosis	6.41
Skewness	1.95
Range	41
Minimum	10
Maximum	51
Sum	5317.52
Count	350
Confidence Level(95.0%)	0.59

<i>TLS DBH</i>	
Mean	15.08
Standard Error	0.29
Median	13.5
Mode	10
Standard Deviation	5.47
Sample Variance	29.88
Kurtosis	7.14
Skewness	2.04
Range	40.8
Minimum	10
Maximum	50.8
Sum	5276.98
Count	350
Confidence Level(95.0%)	0.57

Appendix 4: AGB derived from TLS using general and specific wood density.

<i>TLS_AGB default/generic wood density</i>		<i>TLS_AGB using specific wood density</i>	
Mean	92.79	Mean	114.50
Standard Error	7.10	Standard Error	9.05
Median	64.36	Median	74.98
Standard Deviation	75.78	Standard Deviation	96.66
Sample Variance	5743.08	Sample Variance	9343.18
Kurtosis	2.62	Kurtosis	4.13
Skewness	1.65	Skewness	1.89
Range	363.27	Range	527.63
Minimum	20.98	Minimum	28.26
Maximum	384.25	Maximum	555.89
Sum	10577.89	Sum	13053.10
Count	115	Count	115
Confidence Level(95.0%)	14.06	Confidence Level(95.0%)	17.94

Appendix 5: t-test is assuming two samples of equal variance.

	<i>Field_AGB kg/tree (SWD)</i>	<i>Field_AGB kg/tree (generic)</i>
Mean	116.86	94.59
Variance	9338.44	5789.68
Observations	114	114
Pooled Variance	7564.06	
df	226	
t Stat	1.93	
P(T<=t) one-tail	0.03	
t Critical one-tail	1.65	
P(T<=t) two-tail	0.05	
t Critical two-tail	1.97	

Appendix 6: t-test is assuming two samples of equal variance for AGB derived from TLS.

	<i>TLS_AGB kg/tree(SWD)</i>	<i>TLS_AGB kg/tree (generic)</i>
Mean	114.50	92.79
Variance	9343.18	5743.08
Observations	114	114
Pooled Variance	7543.13	
df	226	
t Stat	1.89	
P(T<=t) one-tail	0.03	
t Critical one-tail	1.65	
P(T<=t) two-tail	0.06	
t Critical two-tail	1.97	

Appendix 7: t-test assuming two samples of equal variance

	<i>QSM_AGB kg/tree (SWD)</i>	<i>QSM_AGB kg/tree (generic)</i>
Mean	122.92	90.76
Variance	10828.76	5890.08
Observations	114	114
Pooled Variance	8359.42	
df	226	
t Stat	2.66	
P(T<=t) one-tail	0.00	
t Critical one-tail	1.65	
P(T<=t) two-tail	0.01	
t Critical two-tail	1.97	

Appendix 8: t-test that shows the relation between AGB estimated by TLS derive tree parameters and QSM derived volume using generic(a) and specific wood density(b)

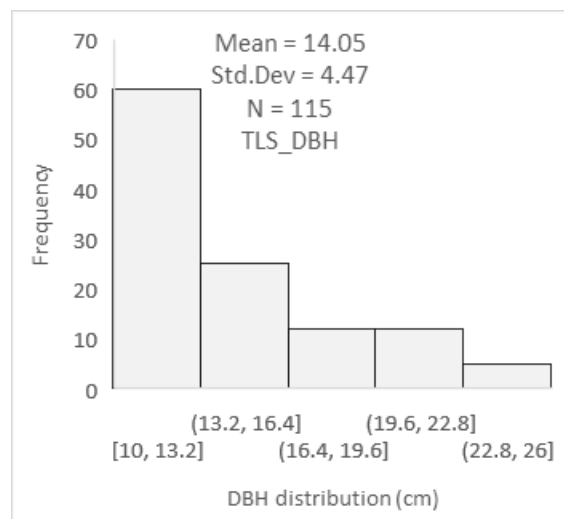
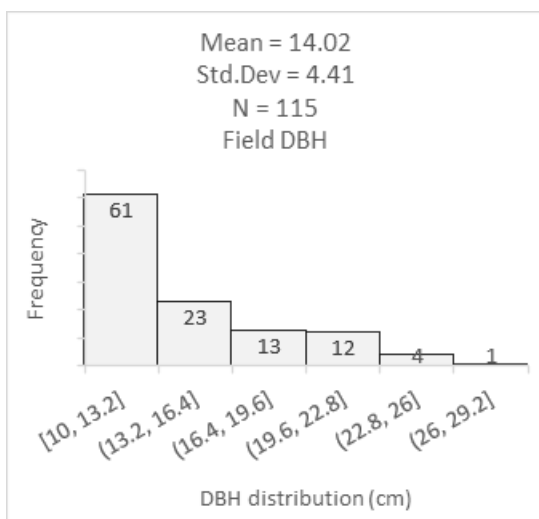
	<i>TLS_AGB (kg/tree)</i>	<i>QSM_AGB (kg/tree)</i>
Mean	92.79	90.76
Variance	5743.08	5890.08
Observations	114	114
Pooled Variance	5816.58	
df	226	
t Stat	0.20	
P(T<=t) one-tail	0.42	
t Critical one-tail	1.65	
P(T<=t) two-tail	0.84	
t Critical two-tail	1.97	

(a)

	<i>QSM_AGB (kg/tree)</i>	<i>TLS_AGB (kg/tree)</i>
Mean	122.92	114.50
Variance	10828.76	9343.18
Observations	114	114
Pooled Variance	10085.97	
df	226	
t Stat	0.63	
P(T<=t) one-tail	0.26	
t Critical one-tail	1.65	
P(T<=t) two-tail	0.53	
t Critical two-tail	1.97	

(b)

Appendix 9. positive skewness of DBH form field and TLS



Appendix 10: t-test of DBH and height from field and TLS left to right.

	<i>Field DBH (cm)</i>	<i>TLS DBH (cm)</i>		<i>Field height (m)</i>	<i>TLS height (m)</i>
Mean	15.15	15.08	Mean	13.11	12.76
Variance	30.36	29.82	Variance	6.92	7.36
Observations	350	350	Observations	350	350
Pooled Variance	30.09		Pooled Variance	7.14	
df	698		df	698	
t Stat	0.15		t Stat	1.74	
P(T<=t) one-tail	0.44		P(T<=t) one-tail	0.04	
t Critical one-tail	1.65		t Critical one-tail	1.65	
P(T<=t) two-tail	0.88		P(T<=t) two-tail	0.08	
t Critical two-tail	1.96		t Critical two-tail	1.96	

Appendix 11: t-test form field and TLS using specific and generic wood density left to right.

	<i>Field_AGB (kg/tree)</i>	<i>TLS_AGB (kg/tree)</i>		<i>Field_AGB (kg/tree)</i>	<i>TLS_AGB (kg/tree)</i>
Mean	116.86	114.50	Mean	94.59	92.79
Variance	9338.44	9343.18	Variance	5789.68	5743.08
Observations	114	114	Observations	114	114
Pooled Variance	9340.81		Pooled Variance	5766.38	
df	226		df	226	
t Stat	0.18		t Stat	0.18	
P(T<=t) one-tail	0.43		P(T<=t) one-tail	0.43	
t Critical one-tail	1.65		t Critical one-tail	1.65	
P(T<=t) two-tail	0.85		P(T<=t) two-tail	0.86	
t Critical two-tail	1.97		t Critical two-tail	1.97	

Appendix 12: t-test from the field and QSM using specific and generic wood density left to right.

	<i>Field_AGB (kg/tree)</i>	<i>SWD QSM_AGB (kg/tree)</i>		<i>Field_AGB (kg/tree)</i>	<i>QSM_AGB (kg/tree)</i>
Mean	116.86	122.92	Mean	94.59	90.76
Variance	9338.44	10828.76	Variance	5789.68	5890.08
Observations	114	114	Observations	114	114
Pooled Variance	10083.60		Pooled Variance	5839.88	
df	226		df	226	
t Stat	-0.46		t Stat	0.38	
P(T<=t) one-tail	0.32		P(T<=t) one-tail	0.35	
t Critical one-tail	1.65		t Critical one-tail	1.65	
P(T<=t) two-tail	0.65		P(T<=t) two-tail	0.71	
t Critical two-tail	1.97		t Critical two-tail	1.97	

Appendix 13. Field photo

